Garini, E. *et al. Géotechnique* [**doi:** 10.1680/geot.9.P.070]

Asymmetric 'Newmark' sliding caused by motions containing severe 'directivity' and 'fling' pulses

E. GARINI*, G. GAZETAS* and I. ANASTASOPOULOS*

Sliding of a rigid mass supported on an inclined, seismically shaking plane serves as a conceptual and computational model for a variety of problems in geotechnical earthquake engineering. A series of parametric analyses are presented in the paper using as excitation numerous near-fault-recorded severe ground motions and idealised wavelets, bearing the effects of 'forward-directivity' and 'fling-step'. Using as key parameters the angle β of the sloping plane (mimicking the sliding surface), as well as the frequency content, intensity, nature and polarity of the excitation, the paper aims at developing a deeper insight into the mechanics of the asymmetric sliding process and the role of key parameters of the excitation. It is shown that 'directivity' and 'fling' affected motions containing long-period acceleration pulses and large velocity steps, are particularly 'destructive' for the examined systems. The amount of accumulating slip on a steep slope is particularly sensitive to reversal of the polarity of excitation. With some special ground motions, in particular (such as the Sakarya and Yarimca accelerograms, both recorded 3 km from the surface expression of the North Anatolian Fault that ruptured in the 1999 Kocaeli earthquake), what might at first glance appear elusively as 'small details' in the record may turn out to exert a profound influence on the magnitude of slippage – far outweighing the effects of peak acceleration, peak velocity and Arias intensity. The results are compiled in both dimensionless and dimensional charts, and compared with classical charts from the literature. Finally, it is shown that no convincingly robust correlation could exist between accumulated slip and the Arias intensity of excitation.

KEYWORDS: earthquakes; embankments; retaining walls; slopes

Le glissement d'une masse rigide soutenue sur un plan vibrant sismiquement est utilisé comme modèle conceptuel et de modélisation pour une série de problèmes en génie antisismique géotechnique. La présente communication comprend une série d'analyses, faisant usage, pour l'excitation, de nombreux mouvements sévères du sol relevés à proximité de la faille et d'ondelettes idéalisées, portant les effets d'une « directivité en avant » et d'un « *fling step* ». En utilisant, comme paramètres clé, l'angle β du plan incliné (en imitant ainsi la surface glissante) et le contenu en fréquence, l'intensité, la nature, et la polarité de l'excitation, la communication s'efforce d'approfondir les connaissances sur la mécanique du processus de glissement asymétrique et le rôle des paramètres clé de l'excitation. Elle démontre que les mouvements affectés par la « directivité » et le « *fling* », contenant des impulsions d'accélération à longue période et des gradins à vitesse élevée, sont particulièrement « destructifs » pour les systèmes examinés. La quantité de glissement cumulé sur une pente raide est particulièrement sensible à l'inversion de la polarité de l'excitation. Notamment, avec certains mouvements du sol particuliers (comme les accélérogrammes de Sakarya et Yarimca, relevés tous les deux à 3 km de l'expression en surface de la faille nord-anatolienne, qui s'est rompue lors du tremblement de terre de Kocaeli, en 1999), ce qui ne semble constituer, au premier abord, que des « *détails de moindre importance* » sur le relevé pourrait en fait influer considérablement sur la magnitude du glissement, en dépassant largement les effets de l'accélération maximale, de la vitesse maximale, et de l'intensité d'Arias. Les résultats sont reportés sur des tableaux dimensionnels et non dimensionnels, et comparés avec des tableaux classiques contenus dans des ouvrages existants. On démontre enfin qu'il ne pourrait exister aucune corrélation suffisamment solide entre le glissement cumulé et l'intensité d'Arias de l'excitation.

INTRODUCTION: ON THE NEWMARK SLIDING BLOCK ANALOGUE AND THE NATURE OF NEAR-FAULT GROUND MOTIONS

The paper addresses the question of what is the practical significance for geotechnical structures of severe 'directivity' and 'fling' pulses such as those usually contained in near-fault ground motions of major seismic events. A major objective of the present paper is to explore the potential of such motions to inflict large irrecoverable deformations on highly inelastic systems, characterised by an asymmetric rigid-plastic restoring force–displacement relationship. Particular emphasis is given to developing a deeper insight into the mechanics of the ensuing inelastic response and to elucidating the role of the nature and sequence of near-fault pulses.

Several applications in geotechnical earthquake engineering require an understanding of the dynamic sliding response of a block of mass m supported on a seismically vibrating base through an *asymmetric* frictional contact. An example is a rigid block of mass, m, resting on a plane inclined at an angle β, as depicted in Fig. 1(a); the available frictional resistance (for excitation acting parallel to the slope) is $F_1 = m\boldsymbol{g}(\mu\cos\beta - \sin\beta)$ when the block slides downward, and $F_2 = m\boldsymbol{g}(\mu\cos\beta + \sin\beta)$ when it moves upward. μ is the *constant* coefficient of Coulomb friction at the block–base interface. Therefore the '*effective*' coefficient of friction for downslope sliding is $\mu_1 = \mu\cos\beta - \sin\beta$, while for upslope sliding it is $\mu_2 = \mu\cos\beta + \sin\beta$.

In his seminal Rankine Lecture, Newmark (1965) proposed that the seismic performance of earth dams and embankments be evaluated in terms of permanent deforma-

Manuscript received 22 May 2009; revised manuscript accepted 15 April 2010.
Discussion on this paper is welcomed by the editor.
* Laboratory of Soil Mechanics, National Technical University, Athens, Greece.

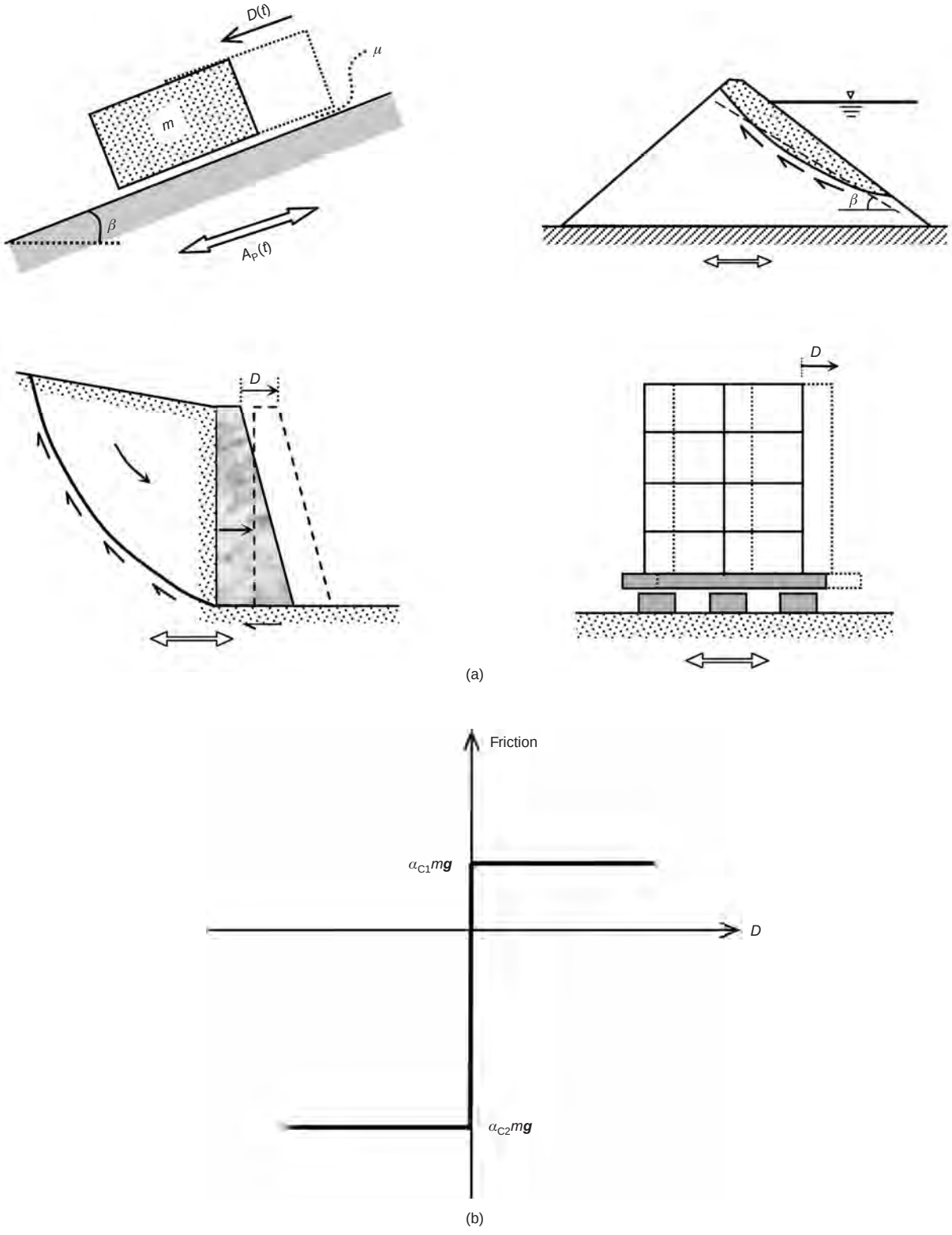

Fig. 1. (a) Schematic representation of the Newmark (1965) sliding-block analogue and potential earthquake engineering applications. (b) Friction force as a function of slip displacement

tions which occur whenever the inertia forces on a potential slide mass are large enough to overcome the frictional resistance at the 'failure' surface (Fig. 1(b)) and he proposed the analogue of *a rigid block on inclined plane* as a simple way of analytically obtaining approximate estimates of these deformations.

Newmark's analogue had been inspired by an earlier unpublished work by R. V. Whitman in connection with the study of the displacements of the Panama Canal slopes if exposed to nuclear explosion – as revealed by Marcuson (1994) and recently reported by Reitherman (2010). Since then, the analogue has seen numerous applications and extensions, three of which are shown in Fig. 1(a). Applications in recent years include the seismic deformation analysis of earth dams and embankments (Seed & Martin, 1966; Ambraseys & Sarma, 1967; Sarma, 1975, 1981; Franklin & Chang, 1977; Makdisi & Seed, 1978; Lin & Whitman, 1983; Constantinou & Gazetas, 1987; Yegian *et al.*, 1991; Sawada

et al., 1993; Gazetas & Uddin, 1994; Kramer, 1996; Kramer & Smith, 1997; Rathje & Bray, 1999); the displacements associated with landslides (Wilson & Keefer, 1983; Jibson, 1994; Harp & Jibson, 1995; Del Gaudio *et al.*, 2003); the seismic deformation of landfills with geosynthetic liners (Bray & Rathje, 1998; Yegian *et al.*, 1998); the seismic settlement of surface foundations (Richards *et al.*, 1993); and the potential sliding of concrete gravity dams (Leger & Katsouli, 1989; Danay & Adeghe, 1993; Fenves & Chopra, 1986). The extension of the analogue by Richards & Elms (1979) to gravity retaining walls has met worldwide acceptance, and has found its way into seismic codes of practice. Several other generalised applications have also appeared (e.g. Constantinou *et al.*, 1984; Ambraseys & Menu, 1988; Ambraseys & Srbulov, 1994; Stamatopoulos, 1996; Rathje & Bray, 2000; Ling, 2001; Fardis *et al.*, 2003; Wartman *et al.*, 2003).

Several of the above studies have utilised a large number of recorded accelerograms to develop design charts, for direct practical application once the '*critical*' (*threshold*) *acceleration* (the term adopted for the '*effective*' *coefficient of friction*) has been pseudo-statically obtained. It appears that, without exception, the available charts (such as those by Sarma (1975), Makdisi & Seed (1978) and Yegian *et al.* (1991), which are widely used in practice) were based on records available in the late 1970s and 1980s. Very few of those motions were near-fault records from large-magnitude ($M > 6{\cdot}5$) events. Today, however, such near-fault records are known often to contain either long-period, high-amplitude acceleration pulses or large residual displacements – the outcome, respectively, either of the *coherent arrival of seismic waves* when the fault rupture propagates towards the site, or of *tectonic permanent displacement* (offset) of the earth in the proximity of the seismogenic fault rupture. The terms 'forward-rupture directivity' and 'fling step' have been given to the two phenomena (Singh, 1985**;** Somerville *et al.*, 1996; Somerville, 2000, 2003; Abrahamson, 2000, 2001; Bolt, 2004). Note one additional consequence of directivity: the components of motion normal to the fault plane are somewhat stronger than those parallel to the fault, especially for periods greater than 0·5 s (Somerville, 2000).

Figure 2 illustrates in idealised form some fundamental characteristics of these two types of near-fault motions. For strike–slip earthquakes, the 'signature' of forward rupture directivity appears in the direction *normal* to the fault, whereas the fling step is significant in the *parallel* component of motion in close proximity to the fault, especially if the latter emerges on the surface with a large static offset. The two phenomena (and directivity in particular) have been the subject of seismological (theoretical and instrumental) as well as earthquake engineering research.

The deeper nature of the two phenomena has been investigated analytically in a seminal paper by Hisada & Bielak (2003), who made use of the representation theorem and paid special attention to the contribution of *static* and *dynamic* Green's functions. They show that fling effects (being of a *static* nature) attenuate very rapidly with distance from the fault, on the order of r^{-2}. That is why fling effects are hardly noticeable with 'buried' faults, whose rupture does not reach close to the ground surface. By contrast, forward directivity effects are the result of constructive wave interference**;** hence, the associated attenuation away from the fault is much slower, of an order which ranges from r^{-1} to $r^{-1/2}$.

Other numerical seismic source models in combination with Green's functions have also been developed, accounting in a natural way for directivity effects (e.g., Pitarka *et al.*, 2000, 2002).

In the aftermath of the Northridge 1994 and Kobe 1995 earthquakes, Somerville *et al.* (1997), having demonstrated that rupture directivity effects cause spatial and directional variations in ground motion at periods beyond 0·6 s, developed improved empirical attenuation relations to account for such effects on strong motion amplitudes and durations. More recent efforts to develop empirical predictive relations and parameter characterisation of the directivity and fling-related pulses include those of Abrahamson (2000), Bray & Rodriguez-Marek (2004), Xie *et al.* (2005), Voyagaki *et al.* (2008a, 2008b), and Taflampas (2009). At the same time the idealisation and mathematical representation of near-fault pulses has attracted significant interest – see Makris & Roussos (2000), Mavroeidis & Papageorgiou (2003, 2010), Howard *et al.* (2005) and Xie *et al.* (2005), among others.

Numerous studies have been published to date assessing analytically and experimentally the potential of 'directivity' pulses to cause large response and inflict damage to a variety of structural systems – the latter falling mostly in the realm of elastic or elastoplastic response (e.g. Bertero, 1976; Bertero *et al.*, 1978; Hall *et al.*, 1995; Gazetas, 1996; Alavi & Krawinkler, 2000; Iwan *et al.*, 2000; Sasani & Bertero, 2000; Junwu *et al.*, 2004; Mavroeidis *et al.*, 2004; Pavlou & Constantinou, 2004; Makris & Psychogios, 2006; Changhai *et al.*, 2007). However, studies on the 'destructiveness' of ground motions containing 'fling-step' pulses have been, understandably, quite limited because the phenomenon has been clearly identified and distinguished from other phenomena only recently (Abrahamson, 2001; Hisada & Bielak, 2003; Xu *et al.*, 2006). Moreover, since the dominant periods of fling-steps are quite long, usually exceeding 2 s, it was presumed (on the basis of the elastic-response way of thinking) that their effects might be less important than directivity effects (Howard *et al.*, 2005). It will be shown in the sequel that with strongly inelastic systems, such as the ones examined here, this may not necessarily be the case at all.

In this paper an idealised rigid-perfectly-plastic system was studied: the block is on a sloping base, the asymmetric sliding of which is governed by Coulomb's friction 'law' with a constant coefficient μ. In addition to the obvious use of the presented results in a number of real-life seismic geotechnical problems (as portrayed in Fig. 1), the examined block-on-inclined-plane model is representative of systems with highly inelastic behaviour. It will be shown that such systems are in fact particularly sensitive to both 'directivity' and 'fling'-related pulses – far more so than are elastic systems.

In a recent paper (Gazetas *et al.*, 2009), the authors have investigated the response of sliding blocks on a *horizontal* plane and on a 25° sloping plane subjected to an idealised motion ('Ricker wavelet') and four actual accelerograms. These motions were applied either horizontally or in a direction parallel to the inclined plane, with or without a simultaneous vertical component of motion. Several important observations were made, focusing on the unpredictable effects of even small 'details' in the records containing 'fling' or 'directivity' pulses. It was revealed that even the strongest *simultaneous vertical excitation* has no discernible effect on either the maximum or the accumulated residual slip – a significant result, which was observed in all cases without exception. This result refutes the prevailing misconception that the role of the vertical component of acceleration is significant for sliding systems (see e.g. Huang *et al.*, 2001), while it renders meaningless the practice of vectorially combining horizontal and vertical peak acceleration values. Sarma & Scorer (2009) have recently arrived at the exact same conclusion regarding the insignificance of the vertical acceleration component on sliding deformation of slopes.

The present paper extends the above work by studying the effects of 23 near-fault accelerograms and four idealised wavelets on the accumulated slip of a rigid block on a plane

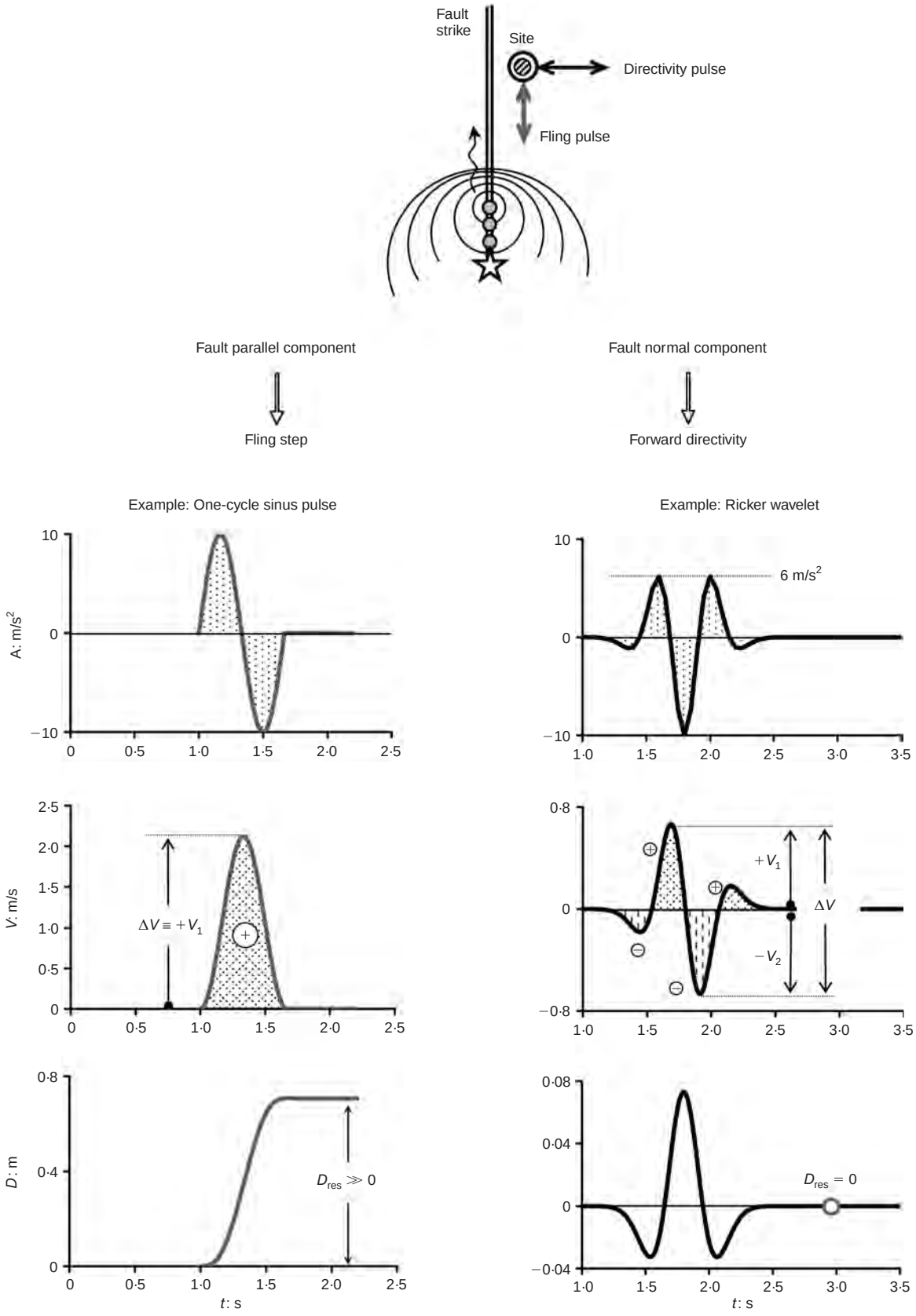

Fig. 2. Schematic explanation of the 'fling-step' and 'forward-directivity' phenomena as reflected in the two sets of idealised acceleration, velocity and displacement–time histories

base inclined at an angle β°. A list of these records and wavelets is given in Table 1 along with some of their key properties. By parametrically varying β from 5° to 25°, the influence of the degree of asymmetry on slippage is assessed. In addition to significant insight that is hoped to be gained from the individual detailed analyses, the results are collectively compared with classical charts from the literature (Sarma, 1975; Makdisi & Seed, 1978; Yegian *et al.*, 1991). A limited set of individual results are developed here in detail.

Table 1. List of significant earthquake records bearing the effects of 'directivity' and 'fling', utilised as excitations in this study

Earthquake, magnitude	Record name	Distance to fault*: km	PGA: g	PGV: m/s	PGD†: m	I_A: m/s
Kobe in 1995,	JMA – 0°	2	0·830	0·810	0·177	8·4
$M_W = 7{\cdot}0$	JMA – 90°	2	0·599	0·761	0·199	5·4
$M_{JMA} = 7{\cdot}2$	Fukiai	3	0·763	1·232	0·134	6·7
	Takatori – 0°	4	0·611	1·272	0·358	8·7
	Takatori – 90°	4	0·616	1·207	0·328	8·1
	Takarazuka – 0°	3	0·693	0·682	0·274	3·1
	Takarazuka – 90°	3	0·694	0·853	0·167	3·9
Erzincan in 1992, $M_S = 6{\cdot}9$	Erzincan (No 95) – EW	2	0·496	0·643	0·236	1·7
	Erzincan (No 95) – NS	2	0·515	0·839	0·312	1·5
Imperial Valley in 1979,	No. 4 – 140°	4	0·485	0·374	0·201	1·3
$M_W = 6{\cdot}8$	No. 4 – 230°	4	0·360	0·765	0·591	0·9
	No. 6 – 140°	1	0·410	0·649	0·276	1·5
Chi-Chi in 1999, $M_w = 7{\cdot}5$	TCU 068 – NS	1	0·353	2·892	8·911	3·3
	TCU 068 – EW	1	0·491	2·733	7·149	3·2
	TCU 102 – NS	2	0·168	0·705	1·062	1·6
Landers in 1992, $M_w = 7{\cdot}2$	Lucerne – 275°	1	0·721	1·360	1·182	6·5
Kocaeli in 1999, $M_w = 7{\cdot}4$	Sakarya – EW	3	0·330	0·814	2·110	1·2
	Yarimca – 60°	3	0·231	0·906	1·981	1·3
San Fernando in 1971, $M_S = 6{\cdot}7$	Pacoima dam – 164°	3	1·226	1·124	0·361	8·9
Northridge 1994, $M_w = 6{\cdot}8$	Rinaldi – 228°	3	0·837	1·485	0·261	7·4
	Jensen Filtration – 22°	3	0·424	0·873	0·265	2·6
	Newhall – 360°	8	0·589	0·753	0·182	5·7
	Sylmar – 360°	4	0·843	1·027	0·256	5·0

Note: PGA, peak ground acceleration; PGV, peak ground velocity; PGD, peak ground displacement
* Approximate closest distance from the actual ruptured (seismogenic) fault, that is r_{rup} according to the definition of the Abrahamson & Shedlock (1997).
† Final ground displacements of the fling-affected records are in accord with Boore (2001).

The term 'severe', appearing even in the title of the present paper, is meant to emphasise the selection of near-fault motions that contain 'deleterious' pulses: either of large duration, or of high amplitude, or both.

ANALYSIS

The analysis of the response of a block of mass m when its supporting base is subjected to motion $A_p(t)$ parallel to its plane, is a straightforward application of Newton's law of motion along with rigid-body kinematics. It is a process well understood and only a bare minimum is discussed here. Knowing the critical accelerations A_{C1} and A_{C2}, and the excitation time history $A_p(t)$, the slip in each sliding stage (downslope or upslope) is easily computed. Thanks to the transient nature of earthquake loading, even if the base were to experience a number of acceleration pulses, in the + or − direction, higher than the critical values α_{C1} or α_{C2}, respectively, this would simply lead to *finite* sliding displacements, downslope or upslope. For small values of the angle β, when A_{C2} is not much larger than A_{C1}, it is quite possible that slip may occur in both directions – the final residual D_{res} may thus be smaller than the maximum slip, D_m, from a single pulse. For larger β angles $A_{C2} >> A_{C1}$, and hence sliding will occur only downhill; the finally accumulated residual slip will be simply the sum of the individual slip-steps.

Detailed solutions in the paper are portrayed in a graphical, easily understandable form. Shown below is how this graphical representation makes it straightforward to visualise the errors in some solutions to the problem that have 'leaked' in the published literature, even in recent years.

PARAMETRIC RESULTS: IDEALISED EXCITATION

Four idealised 'wavelets' have been used as the parallel excitation. Illustrated in Fig. 3, these motions can represent the 'core' of the near-fault records: the strong acceleration or velocity pulses associated with 'directivity' or 'fling'. The parameters that are investigated and shown here are:

(*a*) the ratio of α_{C1}/α_p of the downslope critical acceleration divided by the peak value of the base acceleration ($\alpha_{C1}/\alpha_p = A_{C1}/A_P = 0{\cdot}05–0{\cdot}60$)
(*b*) the slope angle ($\beta = 5–25°$)
(*c*) the dominant frequency of excitation ($f_o = 0{\cdot}5–3$Hz)
(*d*) the influence of polarity (the + or – direction of the excitation (i.e. upslope or downslope)).

Only a limited number of characteristic results are portrayed here.

As a first example, Fig. 4 refers to excitation of a mild ($\beta = 5°$) slope by one cycle of sinus pulse having $A_p = 10$ m/s^2, $V_p = 2$ m/s and $f_o = 1{\cdot}5$ Hz – a motion representative of a strong 'fling' pulse (Abrahamson, 2001). The figure serves two purposes: first, to illustrate graphically the solution to the asymmetric sliding process; and second, to show the influence of α_{C1}/α_p on the amount of slip.

In this case, for $\alpha_{C1}/\alpha_p = 0{\cdot}05$ and $\alpha_{C2}/\alpha_{C1} = 5$ the acceleration of the base starts in the *downward* direction. Since $A_p = 10$ m/s^2 exceeds $A_{C2} = 2{\cdot}5$ m/s^2 an *upward* slippage of the block initiates. During this stage, the block attains a constant acceleration $a = a_{C2}$ and thus develops a linear velocity

$$V = A_{C2}\Delta t$$

When, upon deceleration of the base, its velocity reduces and becomes equal to the block velocity ($V = V_{base} \approx -1{\cdot}1$ m/s, at $\Delta t \approx 1{\cdot}1/2{\cdot}5 \approx 0{\cdot}44$ s from the beginning of sliding, or a total $t = 1{\cdot}44$ s), then the relative motion momentarily stops. But by now the base acceleration has reversed (acts uphill), so the block will slide *downhill* with constant acceleration equal to A_{C1}. The ensuing linear velocity ($V = A_{C1}\Delta t$) will take a greater time, $\Delta t \approx 2{\cdot}3$ s (or total $t \approx 3{\cdot}7$ s), to equalise with the base velocity – that is to vanish, since in this case the base motion soon terminates and no other reversal of

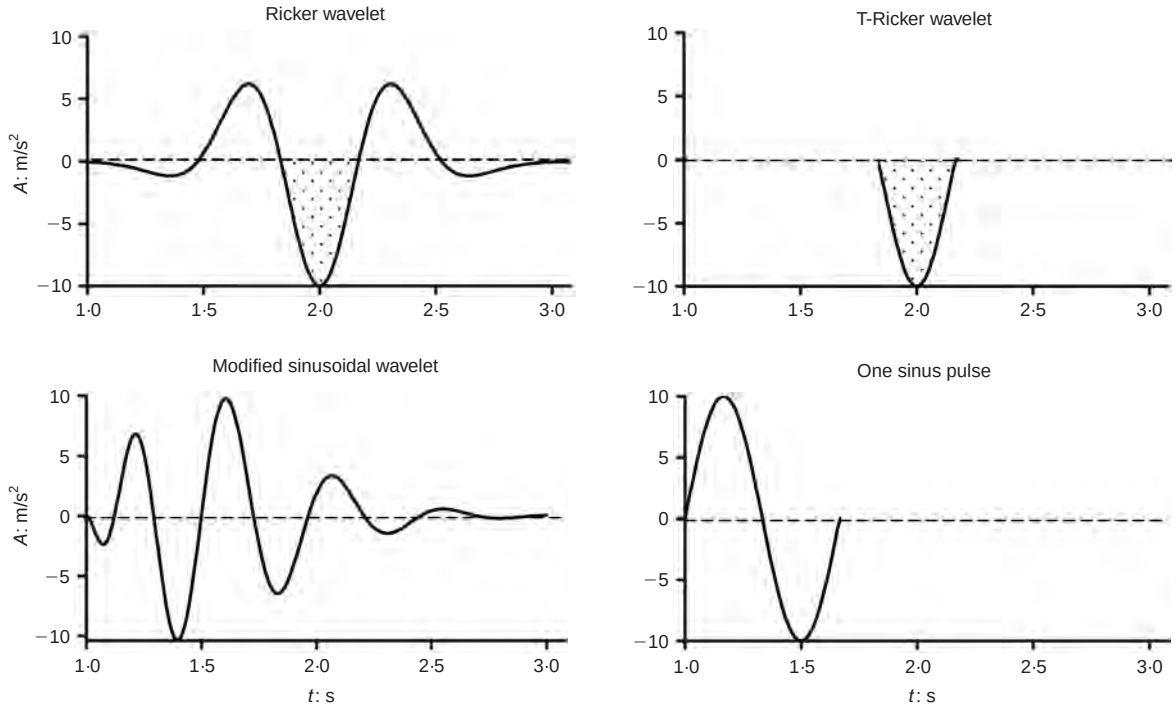

Fig. 3. Idealised wavelets and simple pulses employed as triggering excitations to this study

acceleration takes place. The resulting residual downslope displacement, D_{res}, is $0{\cdot}76\ \text{m} = 1{\cdot}16\ \text{m} - 0{\cdot}40\ \text{m}$, where $D_m = 1{\cdot}16$ m is the total downward slip after the reversal of sliding.

Increasing the α_{C1}/a_C ratio to 0·10 reduces the residual displacement to 0·40 m, although as can be seen in Fig. 4 the upward slip in the first half cycle has only barely decreased compared to the previous case.

The profound effect of excitation frequency has long been established. It is demonstrated here in Fig. 5 with two one-cycle sinus excitations having $f_o = 1{\cdot}5$ Hz and $f_o = 3$ Hz, respectively. Evidently, increasing the frequency reduces the duration of each sliding excursion and thereby the slippage. For the chosen steep slope ($\beta = 25°$) only downslope sliding takes place, leading to a residual slip of 1·10 m, roughly $\frac{1}{4}$ of 4·25. This confirms the well-known conclusion from dimensional analysis that D_{res} is inversely proportional to f_o^2 (Sarma, 1975; Yegian & Lahlaf, 1992; Makris & Psychogios, 2006; Gazetas *et al.*, 2009).

This figure, with the straightforward graphical demonstration of the solution, serves an additional purpose: to point out that erroneous solutions have appeared in the literature in recent years. For instance, Del Gaudio *et al.* (2003) compute the residual slip through the double integral

$$D_{res} = \int_0^{T_d}\int_0^{T_d} [A_p(t) - A_c] \cdot \mathrm{H}\{A_p(t) - A_c\}\ \mathrm{d}t\ \mathrm{d}t \qquad (1)$$

where T_d is the duration of the record and H { } is the Heaviside function. The latter is also called the unit step function, and is a discontinuous function whose value is 0 for negative arguments and 1 for positive arguments. Applied in the case of one-cycle sinus with $f_o = 1{\cdot}5$ Hz, $A_c = A_{c1} = 0{\cdot}05A_p$ and $A_{c2} \approx A_p$, equation (1) yields

$$\overline{D}_{res} \approx \int_{1{\cdot}34}^{1{\cdot}65}\int_{1{\cdot}34}^{1{\cdot}65} \{10\sin[3\pi(t - 1{\cdot}33)] - 0{\cdot}5\}\ \mathrm{d}t\ \mathrm{d}t \qquad (1a)$$

$$\approx 0{\cdot}66\ \text{m}$$

This grossly underestimates (by a factor of about 7) the rigorously computed 4·25 m. The reader can follow using Fig. 5(a) the meaning of the above (inappropriate) integral: in addition to producing wrong residual values, since it completely misses the duration of sliding (which generally has nothing to do with T_d, as seen in Fig. 5), the integral misrepresents the role of consecutive pulses and the role of the negative part of the accelerogram; and of course it cannot possibly recognise the role of some 'significant details' of the ground excitation, the presence of which might have significant repercussions for the sliding block.

A different excitation is utilised for Fig. 6: a Ricker wavelet with $A = 10$ m/s^2 and characteristic frequency $f_o = 1$ Hz – representative of strong 'directivity' affected motions. Two inclinations are compared: $\beta = 5°$ and 25°. For $\alpha_{C1}/a_p = 0{\cdot}05$ only on the flatter (5°) slope does upward sliding occur; the resulting residual slip is about half of the value experienced by the block on the steep (25°) slope.

The surprising significance of changing the motion polarity

The next three figures (Figs 7–9) address an astonishing effect: that of the reversal in polarity (i.e. change from + to − direction in which the excitation is applied). This is the same as having two identical slopes, one opposite to the other ('across the street'), subjected to the same excitation, as illustrated at the top of Figs 7–9.

To the authors' knowledge, few researchers and only in recent years (Fardis *et al.*, 2003; Kramer & Lindwall, 2004) appear to have published on the great importance of the polarity of shaking. The authors believe that this happened so late in the course of development of earthquake geotechnics because little evidence existed on the asymmetry of recorded motions, which is what accentuates the importance of polarity**.** It is mainly the near-fault strong motions that are highly asymmetric due to the contained 'directivity' and 'fling' pulses; but few such motions had been recorded worldwide 20 years ago. Now a large number have become available, hence the aroused interest.

The sliding analysis of Fig. 7 is simple but revealing. For

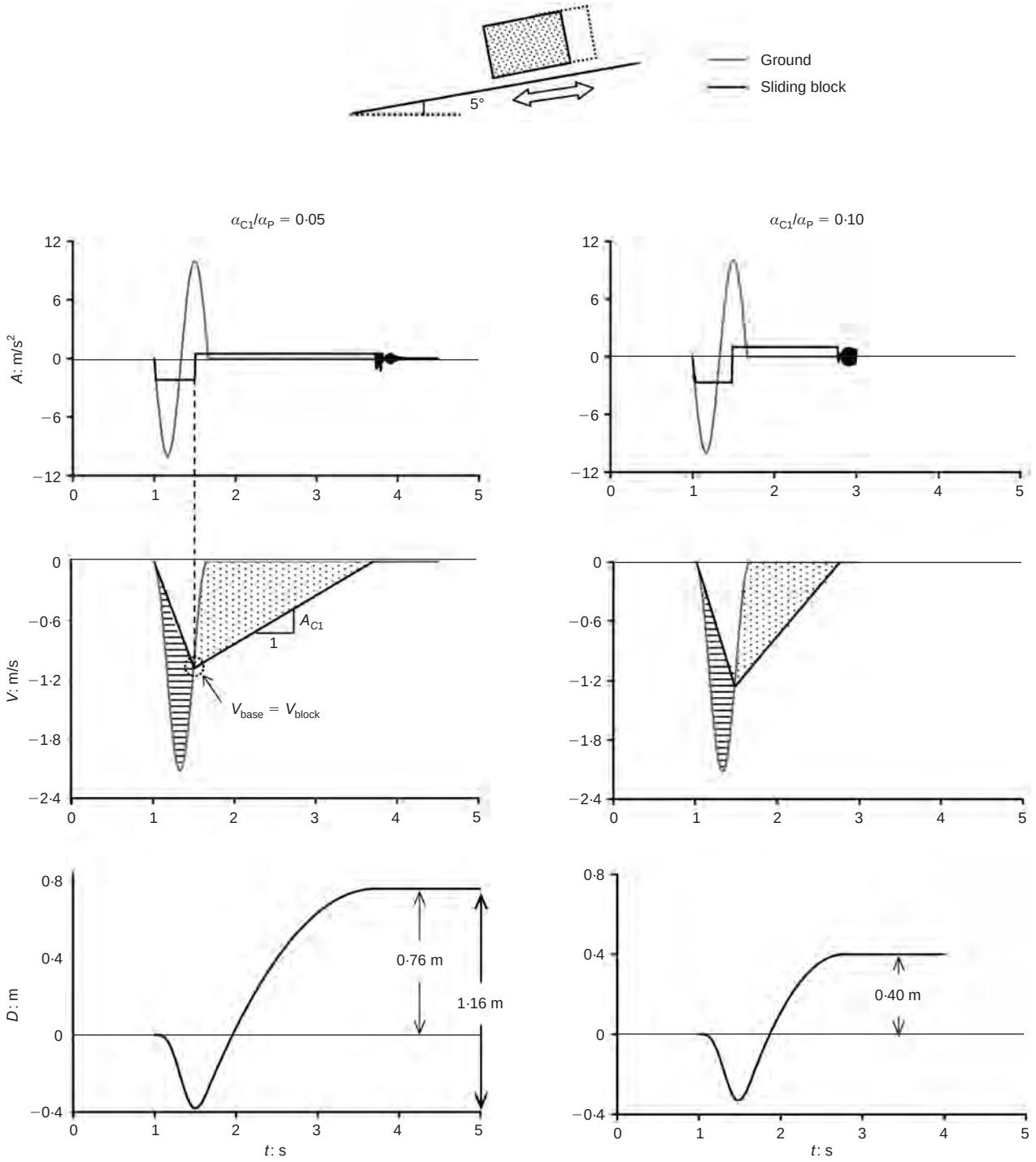

Fig. 4. Acceleration, velocity and sliding displacement–time histories triggered by a one-cycle sinusoidal pulse of $f_o = 1{\cdot}5$ Hz. Effect of acceleration ratio α_{C1}/α_P on the block response. $\alpha_{C1}/\alpha_P = 0{\cdot}05$ for the plots on the left and 0·1 for those on the right. The shaded areas in the velocity–time histories represent the upward (striped) or downward (dotted) sliding

a steep slope ($\beta = 25°$) and a small yield acceleration, $a_{C1}/a_p = 0{\cdot}05$, notice the following: when the first acceleration half-pulse of the base is *downward* (as in Fig. 7(b)) the block remains attached to the base since $a_{C2} \approx a_p$ and no *upslope* slippage initiates; the subsequent, second (and last), *upward* half-pulse acceleration of the base initiates an uninhibited *downslope* slippage of the block, which lasts for a long time after the excitation has terminated – $\Delta t \approx 4{\cdot}2$ s or $t \approx 5{\cdot}7$ s. The result is a huge 4·25 m slip (equal to the dotted, nearly triangular area in the velocity diagram: $\approx 0{\cdot}5 \times 4{\cdot}2 \times 2$).

In stark contrast, when the first acceleration half-pulse of the base is *upward* (as in Fig. 7(a)) the block starts the *downslope* sliding almost immediately (since α_{C1} is very small, only 0·05 α_p). But it soon comes to a stop after about only $\frac{1}{2}$ s, as the *upward* base motion decelerates and then reverses. The resulting residual slip is merely 0·62 m, almost seven times smaller than the 4·25 m produced with the reverse motion.

This readily explainable effect of reversing the polarity of shaking is obviously of profound importance, especially with 'fling'-type motions (as the sinus pulse studied above). It may not, however, be as dramatic with:

(*a*) larger values of critical acceleration ratio, α_{C1}/α_p, as seen in Fig. 8 (for ratios 0·10, 0·20 and 0·40)

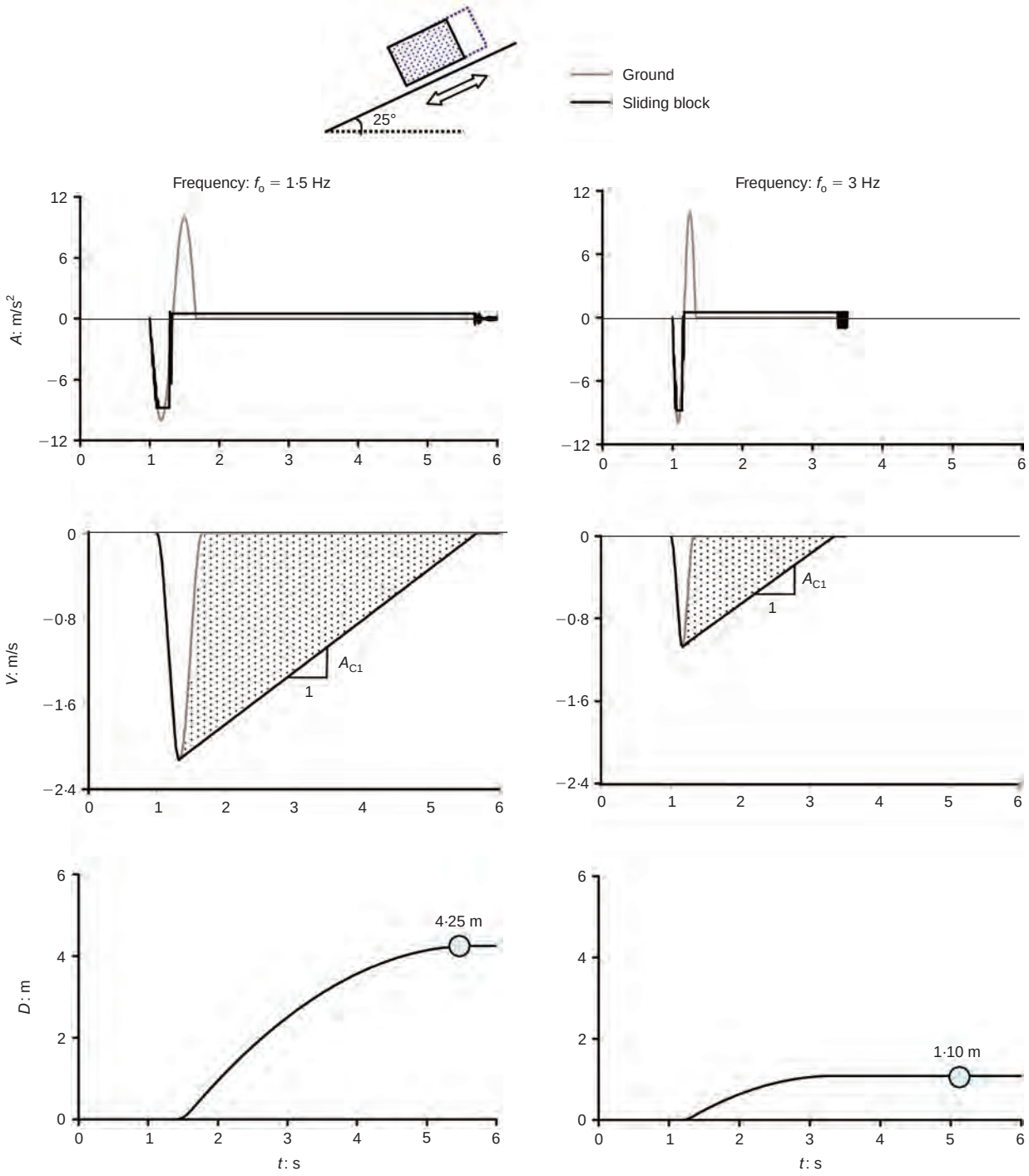

Fig. 5. Acceleration, velocity and sliding displacement–time histories due to a sinusoidal excitation of one cycle, for two different frequencies ($\beta = 25^o$ and $\alpha_{C1}/\alpha_P = 0{\cdot}05$)

(*b*) 'directivity' affected motions if they contain several 'competing' cycles of pulses, as seen in Fig. 9 with the Ricker wavelet
(*c*) milder slopes, as will become evident from subsequent results herein.

PARAMETRIC RESULTS: EXCITATION WITH REAL ACCELEROGRAMS

To verify the above trends (obtained solely with idealised wavelets), analyses with the 23 accelerograms listed in Table 1 are performed. Only a limited number of analyses are shown here in detail, but the results of all analyses are compiled in diagrams and compared with the available charts from the literature.

Figure 10 compares the sliding behaviour of a mass on a 5° and a 25° slope shaken by the directivity-affected Fukiai accelerograms (Kobe earthquake in 1995). The critical acceleration ratio is the same for the two slopes, $\alpha_{C1}/\alpha_p = 0{\cdot}20$, which of course implies a larger coefficient of friction for the steep slope, according to

$$\mu = \tan\beta + \alpha_{C1}/\cos\beta \qquad (2)$$

Notice that on the *mild* (5°) slope the mass undergoes a major downward slip of about 0·48 m after 7 s of shaking, as a result of the acceleration pulse 'c'. There is very little accumulation of slip thereafter, as the high-frequency 'tail'

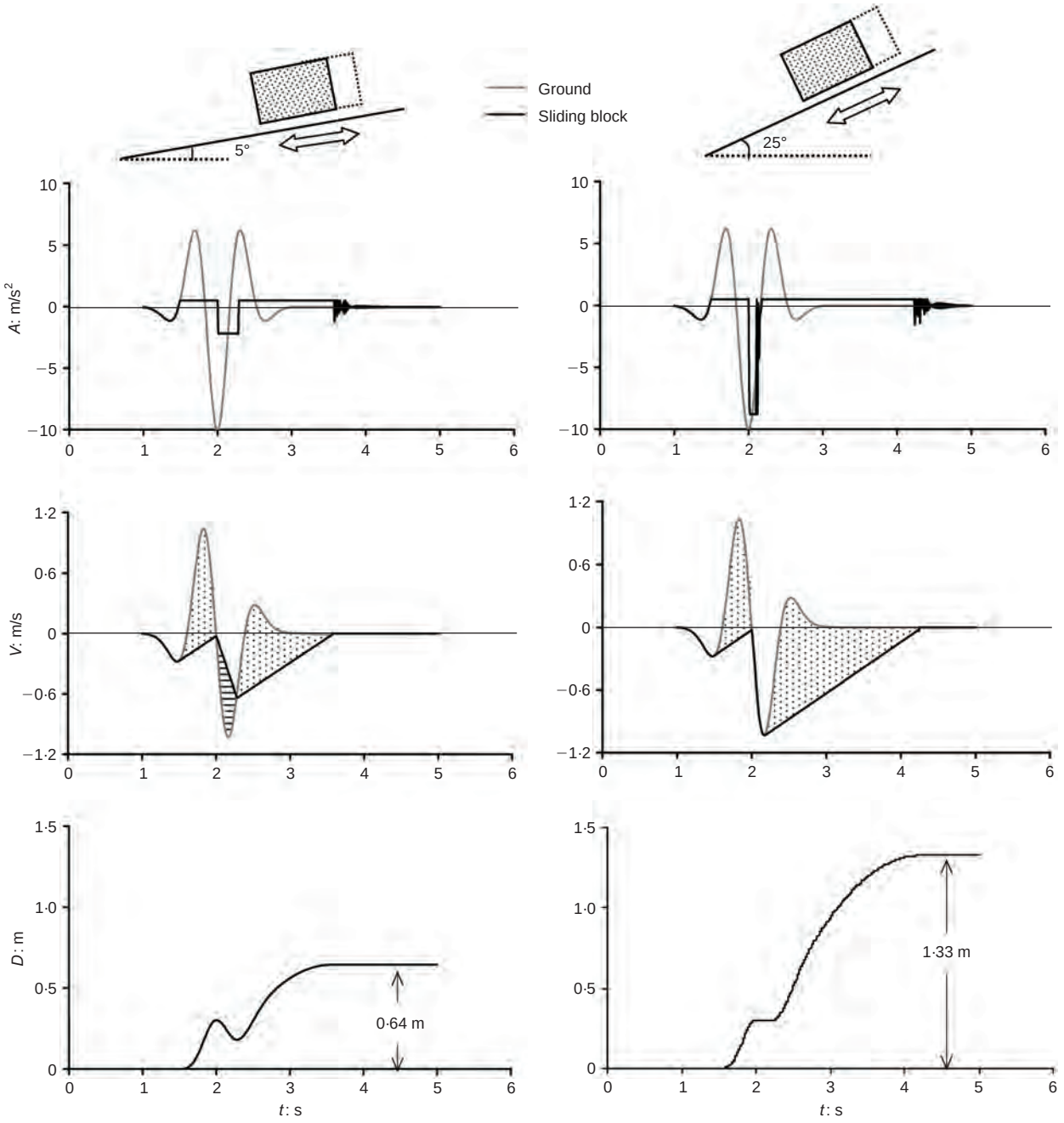

Fig. 6. Effect of slope inclination on the sliding response caused by a Ricker wavelet with $f_o = 1$ Hz and peak acceleration of 1*g*. Acceleration ratio: $\alpha_{C1}/\alpha_P = 0{\cdot}05$. The shaded areas in the velocity–time histories correspond to the downward (dotted) or upward (striped) sliding

of the record leads to negligible sliding, even though the acceleration peaks exceed α_{C1} at least four times. Notice also that pulse 'b' produces an upslope slip of 0·22 m, cancelling out the initial downslope slip stemming from pulse 'a'. Such a beneficial reversal is not observed on the steep (25°) slope ($a_{C2} > a_p$), but otherwise the two downward sliding episodes are almost the same as on the mild slope.

It has become evident by now that the three major pulses (a, b, c), largely the outcome of forward directivity, although of a total duration of barely 3 s, encompass all the potential for slippage of this damaging 10 s record – thus vindicating the use of the idealised pulses (such as the Ricker wavelet) as the simple and readily amenable to parametric investigation surrogates of near-fault motions.

Figures 11–13 compare the sliding–time histories on a horizontal as opposed to a 25°-sloping base, excited respectively by Fukiai, 1995; Takarazuka, 1995; and Sakarya, 1999 – bearing the effects of directivity (1995 records) and of fling-step (1999 record). Three α_{C1}/α_p ratios are considered. Among the noteworthy observations is that even at the very small a_{C1}/a_p *r*atios, 0·05, residual slip on horizontal ground is not excessive (< 0·59 m); it could be acceptable in some applications. By contrast, on the steep slope the accumulated downward slip can be substantial (ranging from 1 m to more than 3 m).

It is interesting to show how the sliding displacements are influenced by the details of the input motion, including the phasing of the various pulses. To this end, Fig. 14 compares the evolution of slippage of a block on a 25° plane excited by two of the most significant records of the Kocaeli 1999 earthquake: the Sakarya-EW and the Yarimca-60° accelerograms. Both were recorded at about 3 km from the ruptured North-Anatolian strike slip fault, which runs almost in the

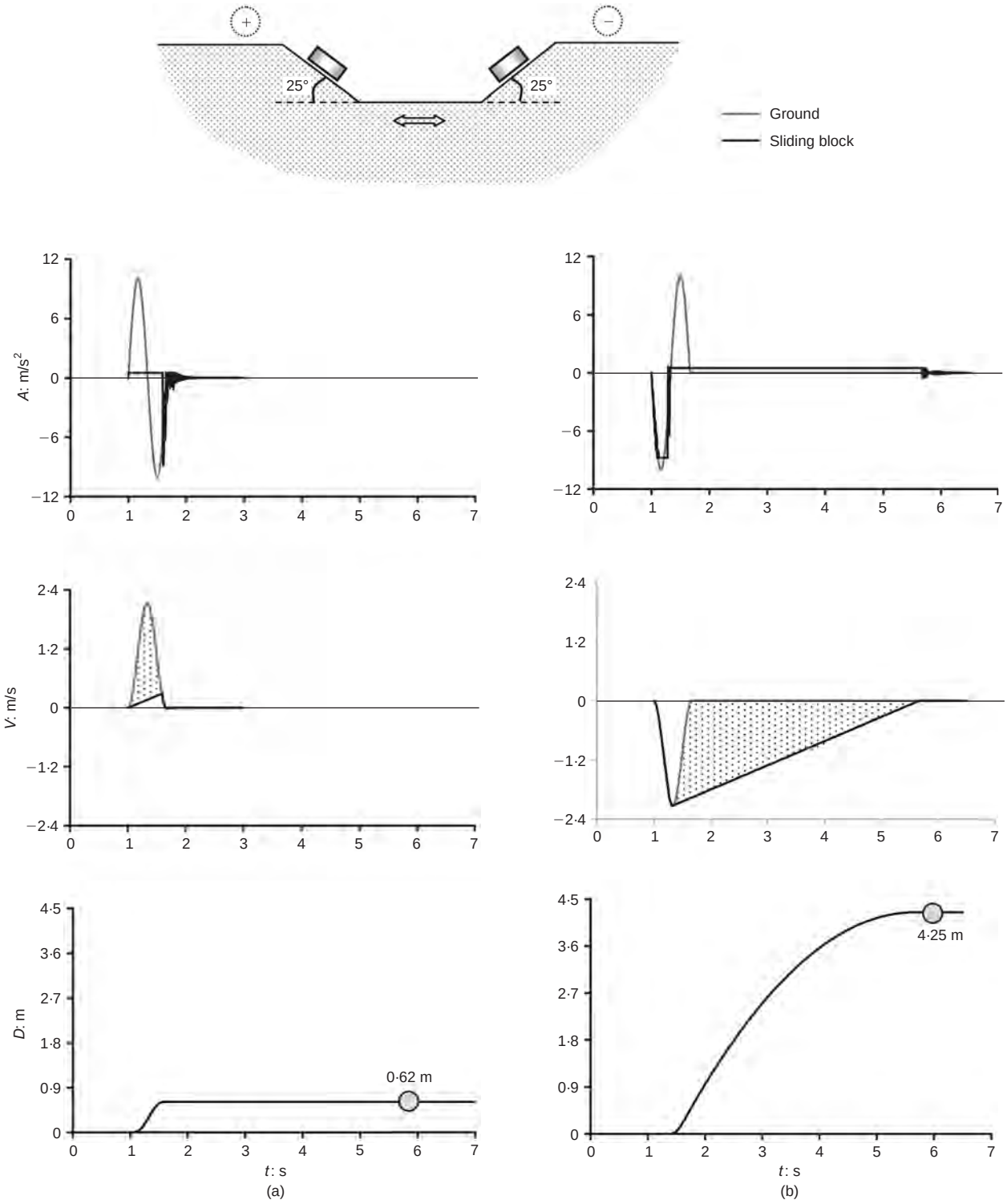

Fig. 7. By reversing the polarity of a one-cycle sinusoidal pulse excitation the resulting slippage increases by a factor of nearly 7 ($\beta = 25^o$, $f_o = 1{\cdot}5$ Hz and $\alpha_{C1}/\alpha_P = 0{\cdot}05$). The sketch on the top is meant to indicate the practical significance of reversed polarity: two identical slopes 'across the street' subjected to identical ground excitation (as would have resulted from vertically propagating shear waves) may have a vastly different performance

east–west direction and emerged on the ground surface not far (≈ 3 km) from the two stations. Evidently, the Sakarya motion, being parallel to the fault bears the 'signature' of its rupture in the form of fling-step: about 2 m of residual (GPS-verified) ground displacement – compared with 3·5–4 m fault offset in the closest outcrop of the fault. The Yarimca-60° contains both directivity- and fling-related pulses.

The two records are quite similar in many respects; they have very similar peak values of peak ground velocity (PGV), peak ground displacement (PGD) and I_A – with the small exception of peak ground acceleration (PGA), which in Yarimca is only about two-thirds of the Sakarya peak value. But despite this 'superiority' in PGA of Sakarya, it is much more benign: it inflicts on the block a far smaller slip (≈ 1 m) than Yarimca ($\approx 4{\cdot}3$ m). The reader can easily discern from the velocity histories the two main culprits of such devastating performance of the system to one and not to the other motion.

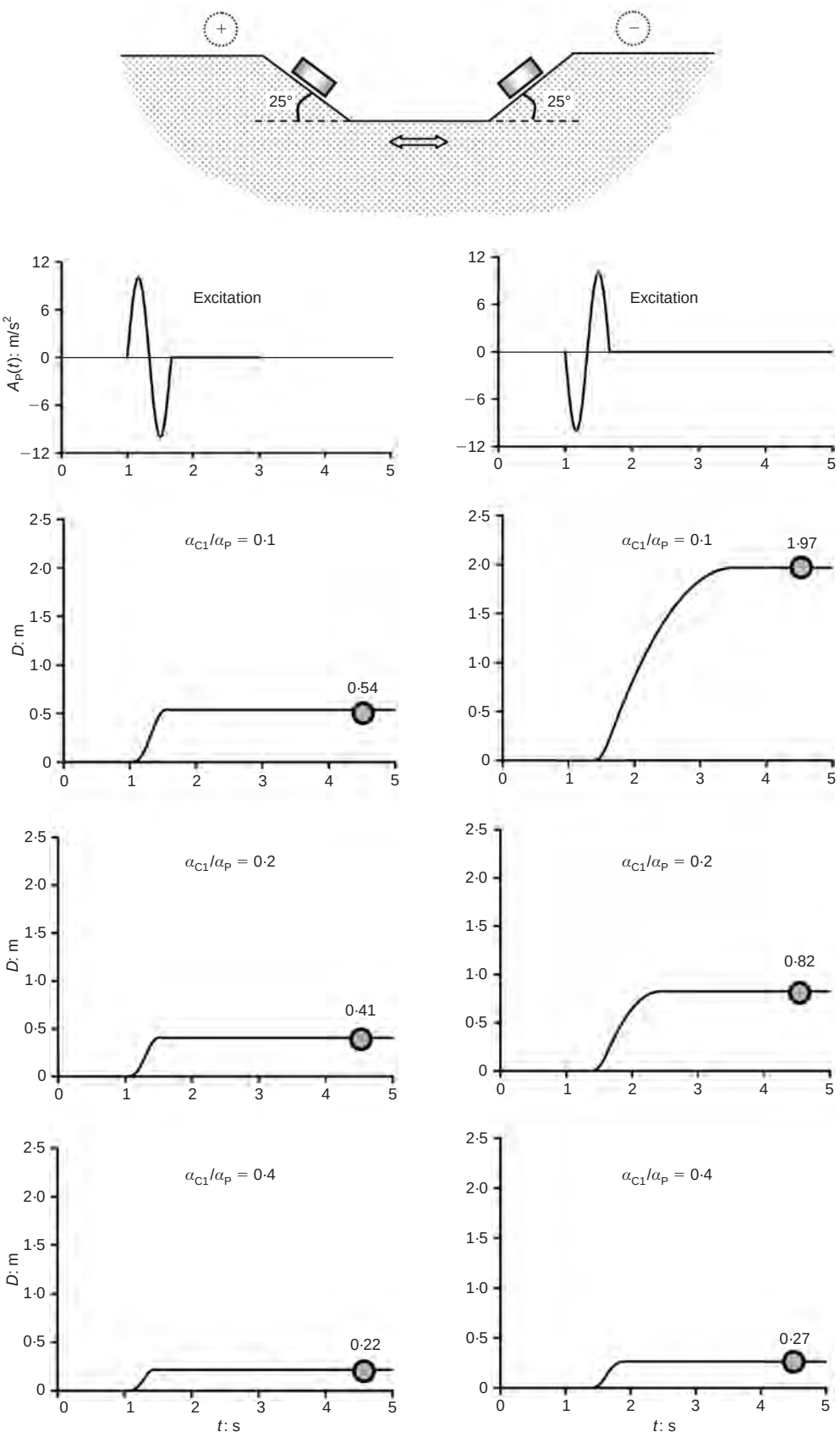

Fig. 8. Effect of reversing polarity of excitation on the asymmetric sliding triggered by a sinusoidal pulse of one cycle with $f_o = 1{\cdot}5$ Hz. Inclination $\beta = 25°$. Observe that the difference in response is large for small values of α_{C1}/α_P, but decreases with increasing α_{C1}/α_P, and practically disappears for $\alpha_{C1}/\alpha_P \geqslant 0{\cdot}5$

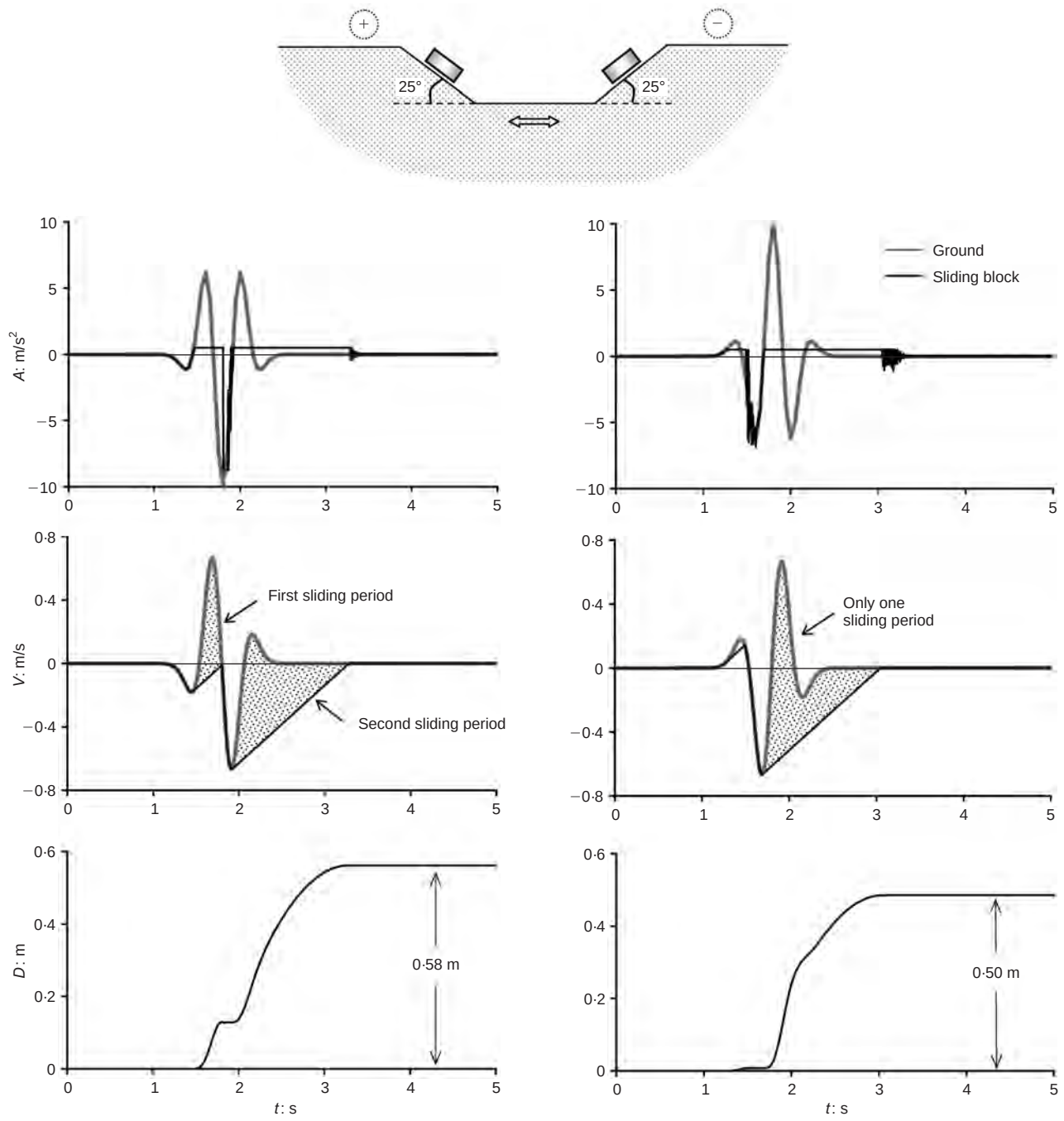

Fig. 9. Effect of reversing the polarity of a Ricker $f_o = 1{\cdot}5$ Hz wavelet, of $f_o = 1{\cdot}5$ Hz, with the peak downward (left) and the peak upward (right): inclination, $\beta = 25°$; acceleration ratio, $\alpha_{C1}/\alpha_P = 0{\cdot}05$. In this case the differences are minor

First, although their PGVs are nearly the same, the velocity steps are quite different: $\Delta V_{Yar} \approx 1{\cdot}4$ m (Yarimca) compared with only $\Delta V_{Sak} \approx 0{\cdot}8$ m (Sakarya). This difference stems from the modest 1 m/s^2 amplitude downward acceleration observed at about 6 s in the Yarimca record. Owing to its relatively long (1·2 s) duration, this acceleration pulse produces a velocity slightly less than what an elementary computation ($\frac{1}{2} \times 1 \times 1{\cdot}2 \approx 0{\cdot}6$ m/s) would have predicted. It is obvious in the figure how this velocity pulse causes the subsequent downward slip to reach 3 m.

Second, after the passage of its main velocity pulse (i.e. for $t > 7$ s) the Sakarya motion did not contain any other important velocity pulses; in stark contrast, the Yarimca motion exhibits one more severe velocity pulse (between about 14 and 17 s) with a step $\Delta V \approx 0{\cdot}65$ m/s, which forces the block to slide an additional 1·3 m – hence to a huge accumulated slip of 4·3 m.

Confirming the 'changing polarity' surprise

In Fig. 15 the excitation is one of the truly remarkable fling-step affected Chi-Chi records: TCU-068. Despite its small peak ground acceleration of 0·34***g***, and in fact quite irrespective of it, the NS component of the record contains a very long duration (≈ 4 s), nearly rectangular pulse of average amplitude ≈ 0·15***g*** after 7 s of motion, and a preceding nearly triangular pulse in the opposite direction, lasting about 2·5 s and having a peak of about 0·20***g***.

It is obvious from Fig. 15 that the effect of changing polarity is significant, perhaps even dramatic. When the 4 s duration pulse acts downhill (Fig. 15(a)) its effect is minor because the mass tends to accelerate uphill; but the pertinent critical acceleration, $\alpha_{C2} \approx 0{\cdot}86$, is far too high and prevents upslope sliding. The result is a downslope $D_{res} = 8{\cdot}81$ m, produced mainly by the first, 2·5 s duration pulse.

Reversing the polarity ((Fig. 15(b) and Fig. 16(a)) causes

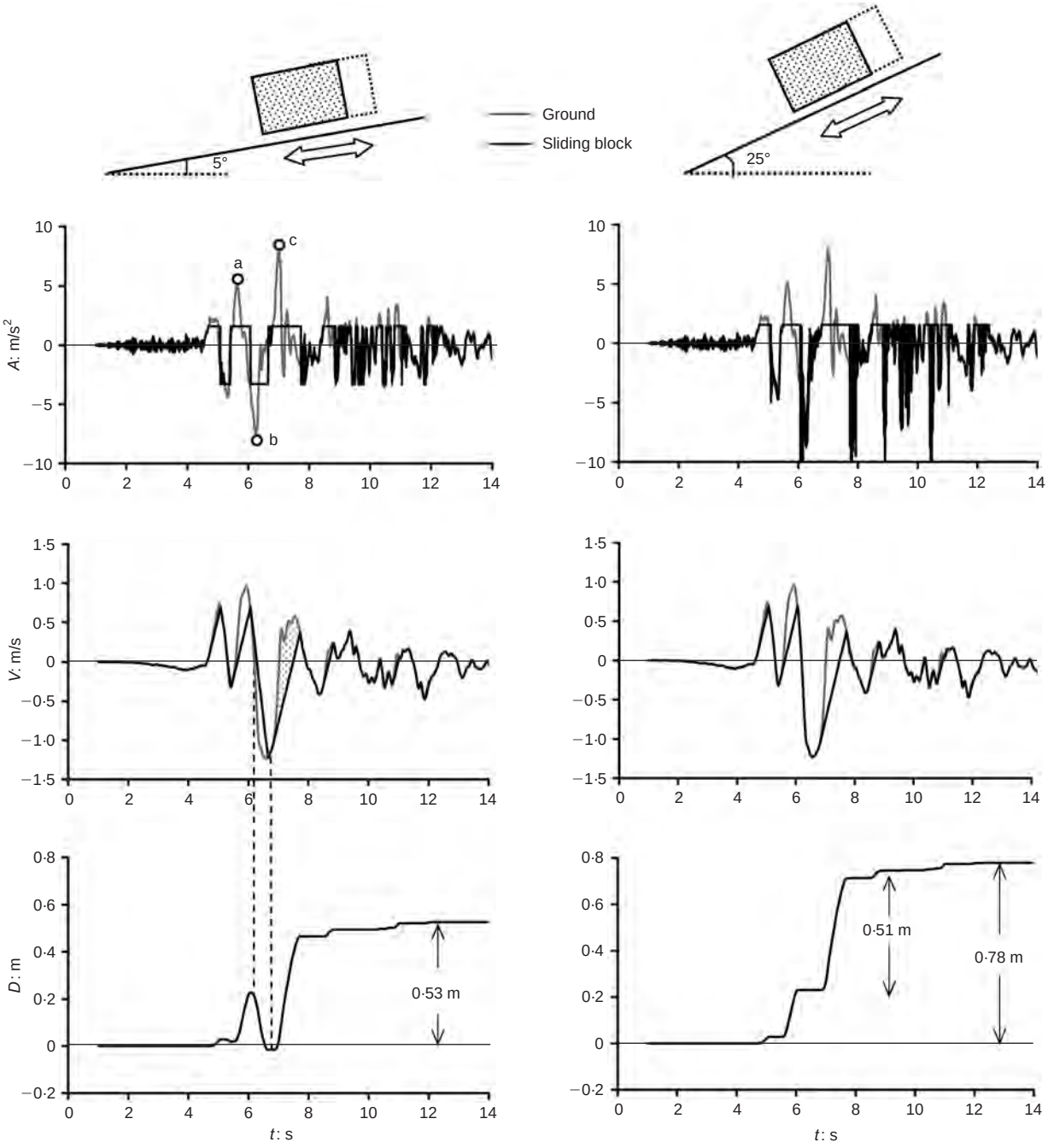

Fig. 10. Effect of slope inclination to asymmetric sliding triggered by the Fukiai ground motion. The plots correspond to a ratio $\alpha_{C1}/\alpha_P = 0{\cdot}2$. In case of $\beta = 5°$, the small inclination allows an uphill sliding of the block

the 4 s duration base pulse to act upward; hence it produces a downslope sliding of the mass which appears to last 'forever'– that is, until the end of the motion ($t = 27$ s). It is hardly surprising therefore that the slip jumps to the colossal 25·3 m.

Significant pulses and their simplified modelling

Figure 16(a) explains in more detail the mechanics of this sliding process. Moreover, it provides an additional proof of the unique importance of the aforesaid long-duration pulse. By eliminating the acceleration high-frequency spikes of the record and crudely approximating the major pulses with rectangles having the same duration and the average acceleration amplitude over that duration, one obtains the grossly simplified time histories, which are plotted in Figs 16(b) and 16(c). Despite the 'innocent' looking peak acceleration of merely $0{\cdot}15\boldsymbol{g}$ of the latter approximation (Fig. 16(c)) this base motion has nearly the same devastating effect on the mass as the real record: a downward slip of 23·3 m (despite the fact that now the α_{C1}/α_p ratio has doubled). The similarity with the effects of the actual motion is obvious, proving the validity of the argument. Incidentally, the more detailed representation of Fig. 16(b), which includes every major acceleration pulse, also leads to very similar sliding response.

Several other important observations have been made with the results of all the motions of Table 1, which cannot possibly be shown here. One finding worth mentioning is that motion features such as the sequence of cycles, and even the 'details' of the motion, are of major importance – sometimes as important as the dominant frequency and the intensity of motion.

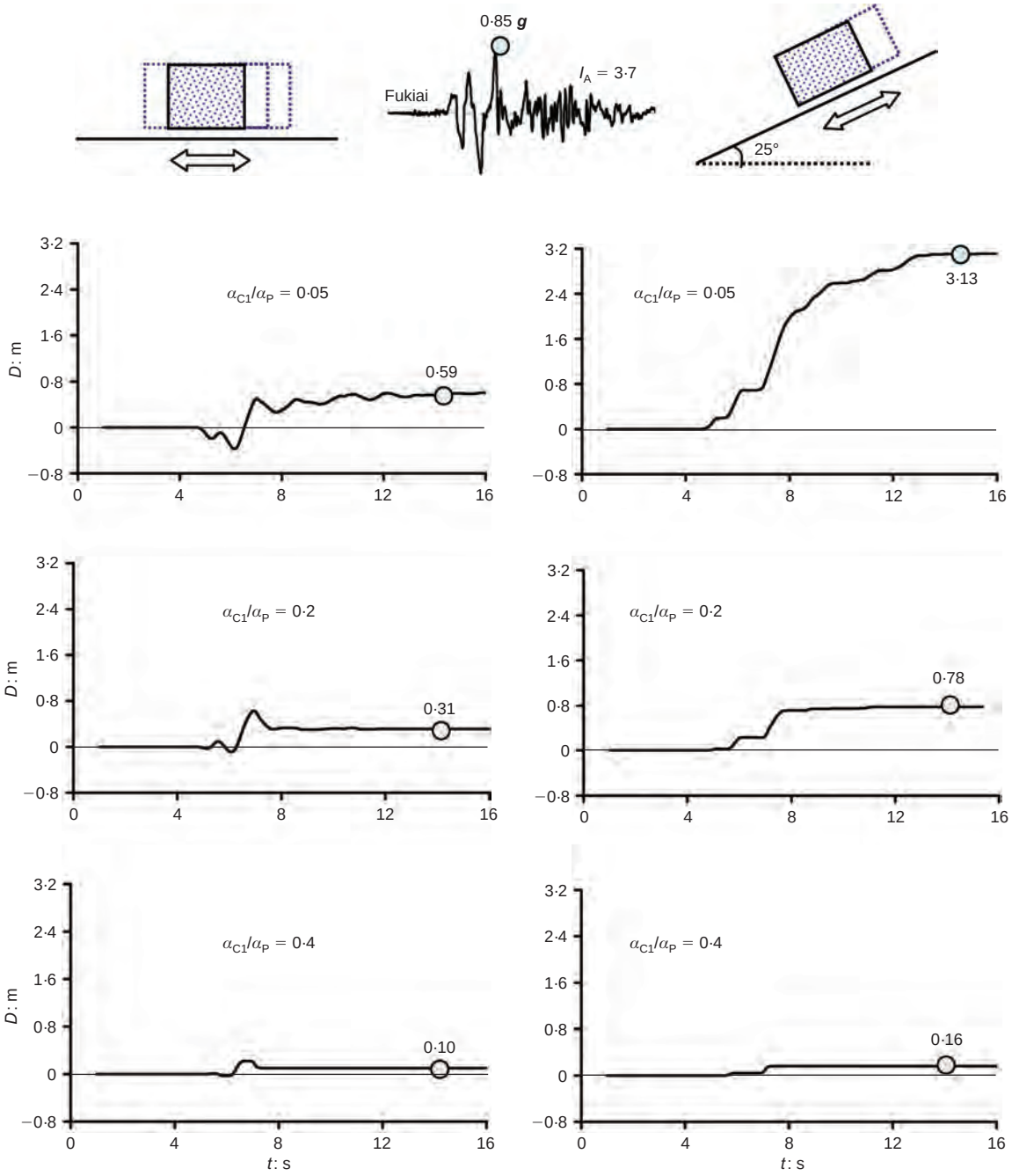

Fig. 11. Influence of the symmetric (left) or asymmetric (right) nature of sliding to the response induced by the Fukiai ground motion

COMPILATION OF ALL RESULTS: COMPARISON WITH AVAILABLE CHARTS

It is of practical interest to compare the results of this study with the relevant charts for sliding displacement published by Makdisi & Seed (1978); Sarma (1975); and Yegian *et al.* (1991). The comparisons are displayed in both dimensionless (Fig. 17) and dimensional (Fig. 18) form. Specifically, Fig. 17 plots the normalised accumulated slip as a function of the critical acceleration ratio

$$\frac{D_{res}}{A_p T_o^2} = f(\alpha_{c1}/\alpha_p) \tag{3}$$

The numerical data points, grouped as those due to idealised wavelets and those due to real accelerograms, are compared in Fig. 17 with the analytical results of Sarma (1975) and in Fig. 18 the 50%-probability-of-non-exceedance curve of Yegian *et al.* (1991).

Figure 19 compares the computed absolute values of the accumulated residual slip (D_{res}) with the Makdisi & Seed (1978) diagram, the scatter of which reflects the huge variability of peak accelerations, velocities, dominant periods and durations in the records that had resulted from earthquake magnitudes: $6{\cdot}5 < M < 7{\cdot}5$. This is the range of magnitudes of the seismic events from which the near-fault records utilised in this work have been distilled. The results are shown for both idealised wavelets (Fig. 19(a)) and real motions; the latter are divided into mainly directivity-affected motions (Fig. 19(b)) and motions mainly containing significant fling-steps (Fig. 19(c)). (It is emphasised that few of the selected records are *purely* directivity or *purely* fling-affected motions.) The following conclusions emerge from Figs 17–19.

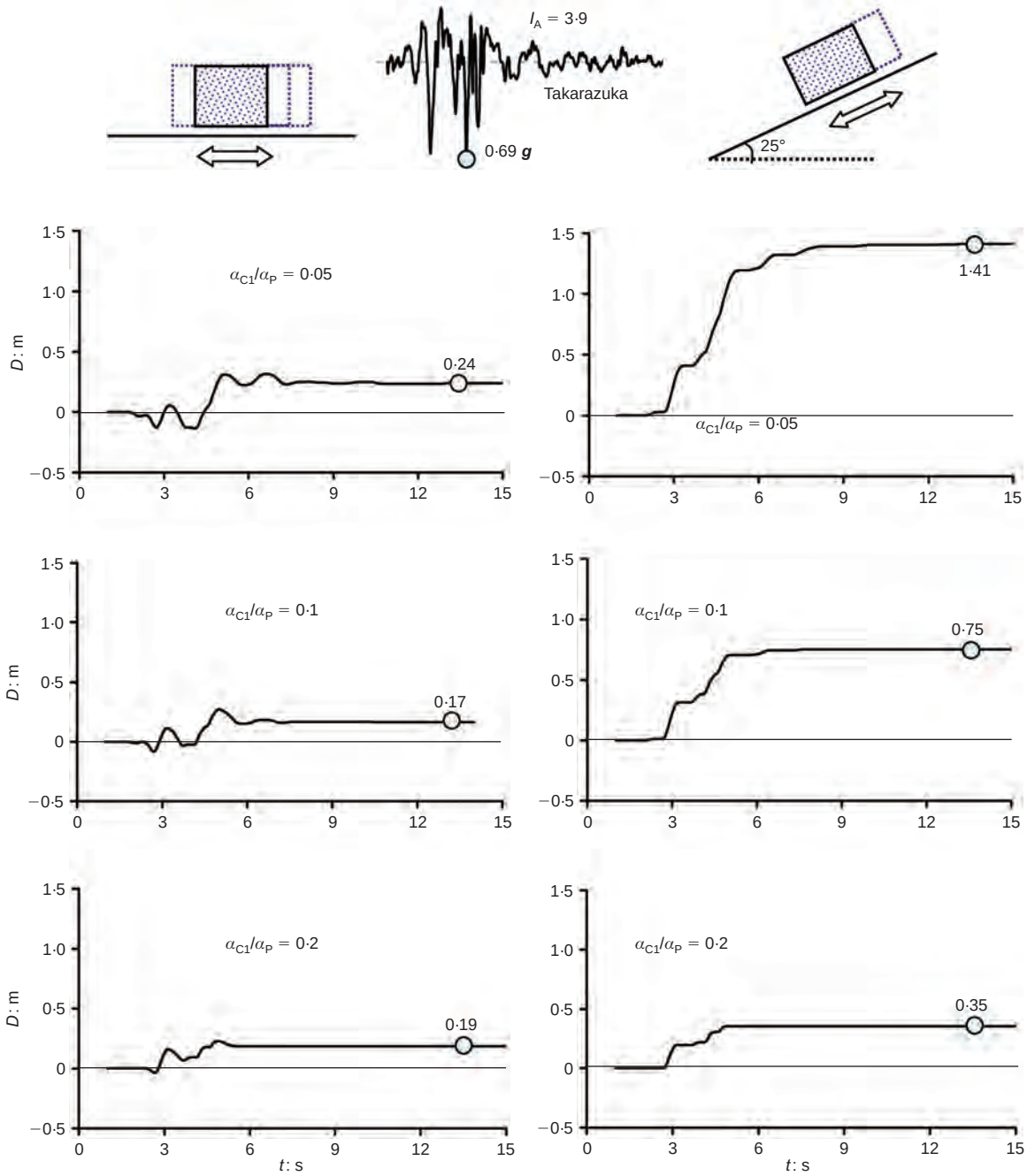

Fig. 12. Influence of the symmetric (left) or asymmetric (right) nature of sliding to the response induced by the Takarazuka-NS ground motion, for three values of α_{C1}/α_P: 0·05, 0·10 and 0·20

(*a*) The dimensionless diagrams derived either for idealised wavelets (Sarma, 1975) or from recorded motions (Yegian *et al.*, 1991) are in accord with the results of the present study.

(*b*) However, both types of actual near-fault records (i.e. fling and directivity affected) may lead to D_{res} values much higher than the upper-bound values of the Makdisi & Seed (1978) curves. Some of the fling-affected motions, in particular, produce slip values that far exceed the highest estimates of Makdisi & Seed (1978).

EMPIRICAL EVIDENCE ON THE ROLE OF 'DIRECTIVITY'

The potential destructiveness of directivity- and fling-affected motions on civil engineering systems has been manifested in many earthquakes: San Fernando in 1971, Northridge in 1994, Kobe in 1995, Aegion in 1995, Kocaeli in 1999, Chi-Chi in 1999 – just to name a few for which well-documented case histories are available in the literature. A few examples are cited below.

The heavy damage of the 'Olive View' hospital during the $M = 6{\cdot}7$ San Fernando earthquake was convincingly attributed (in a thorough study by Bertero, 1976; Bertero *et al.*, 1978) to a long-duration acceleration pulse and the associated large 'velocity step' contained in the ground motion. Although the term 'directivity' was invented later, the explanation of such acceleration and velocity characteristics pointed to forward rupture directivity as the likely mechanism for their generation. The 'soft- first-storey' hospital building, designed to resist acceleration levels much lower than those of the experienced motion, effectively responded in its inelastic range; thus its behaviour resembled that of the rigid-plastic systems examined here. It was located a few

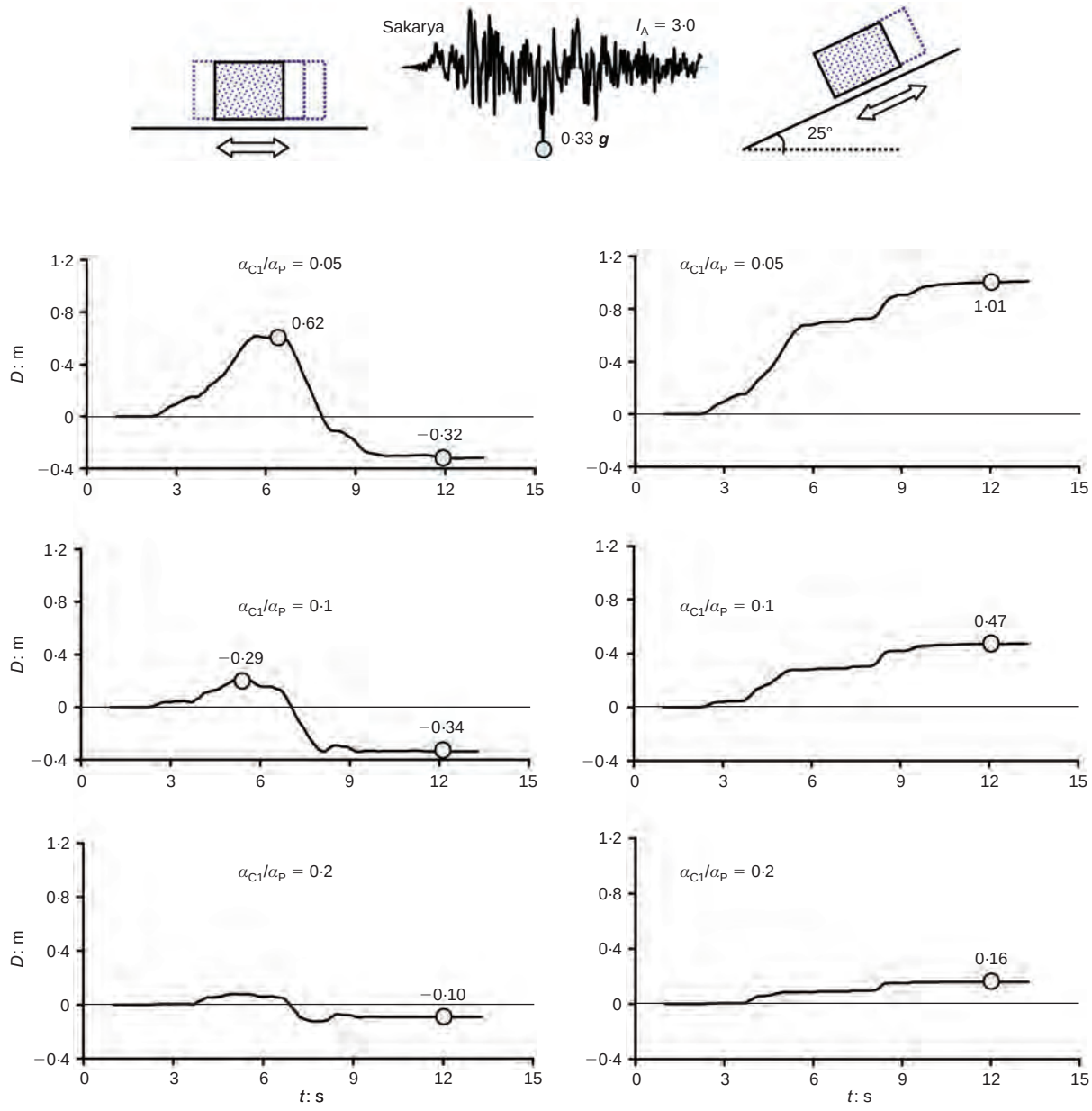

Fig. 13. Symmetric (left) and asymmetric (right) sliding response to the Sakarya ground motion for three values of the α_{C1}/α_P ratio: 0·05, 0·10 and 0·20

kilometres from the surface expression of the fault, towards which the 'thrusting' rupture propagated.

The 1995 $M_{JMA} = 7{\cdot}2$ Kobe earthquake provided an abundance of failures of all types of geotechnical and structural systems, for which directivity played a manifestly principal role. The large sliding–rocking displacements of the harbour retaining (quay) walls in the nearly 200 wharves of the city should in particular be mentioned here. On the two man-made islands, Port and Rokko, not only were the seaward displacements at the top of these walls huge, but they were also a function of the wall orientation: on the island sides, which were nearly parallel to the causative fault, they ranged between 3 and 6 m; on the sides that were nearly perpendicular to the fault they were mostly limited to 1–3 m (Hamada *et al.*, 1995; Hamada & Wakamatsu, 1996; Ishihara, 1997). This difference was attributed to 'forward-rupture directivity' which is known to lead to much larger long-period components of motion in the direction normal to the fault (Somerville, 2000). Since the walls that are parallel to the fault are also perpendicular to these increased components of motion, and thus displace in response to them, they experience much larger sliding and rocking movements. (See Ishihara (1997) and Dakoulas & Gazetas (2008) for some details on the mechanism of quay wall movement.)

ATTEMPTED CORRELATION: RESIDUAL SLIP AGAINST ARIAS INTENSITY

In the (seemingly endless) search of the profession for reliable indexes of 'destructiveness' of ground motions, that is for motion parameters indicative of the severity of a particular shaking, 'Arias intensity' has enjoyed a rather significant popularity. Defined as

$$I_A = (\pi/2\boldsymbol{g})\int_0^\infty \alpha^2(t)\mathrm{d}t \tag{4}$$

it has been correlated with, among other measures of damage, one-directional sliding displacement of rigid blocks

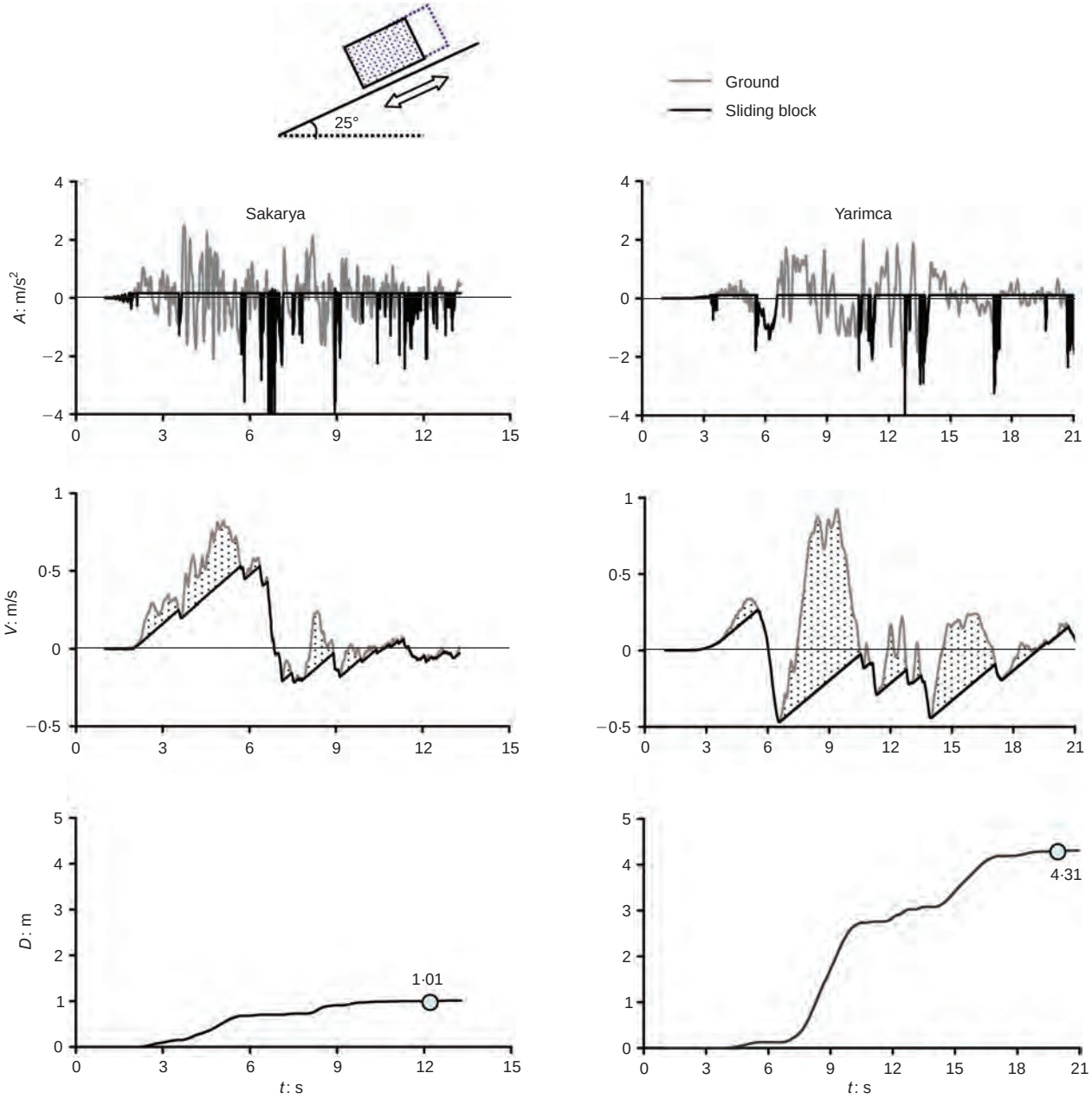

Fig. 14. Acceleration, velocity and displacement time-histories caused by the fling-affected Sakarya record and the directivity-and-fling affected Yarimca-060° record ($\beta = 25°$ and $\alpha_{C1}/\alpha_P = 0{\cdot}05$).

(Jibson, 1994; Kramer, 1996) or flexible slopes (Travasarou, 2003).

An attempt is made here to correlate I_A of the severe near-fault motions utilised in the paper with the permanent slip they produced on a steep (25°) slope. Such permanent (residual) slip is a direct measure of the 'damage' to the respective geotechnical structure (slope, retaining wall, etc.) by the specific excitation.

Figure 20 plots D_{res} (in metres) as a function of the yield acceleration α_{C1} (recall that for $\beta = 25°$, $\alpha_{C1} = \mu \cos 25° - \sin 25°$). No scaling or any other modification to the ground motions was made. The appearance of scatter in the results of each record arises solely from the change in polarity (+ or − direction) of each specific record. The Arias intensity of each motion is written directly on each relevant pair of curves.

Although, admittedly, the presented data in this paper are rather limited for a statistically robust statement, and the selection of 'severe' motions somewhat arbitrary, one can still draw a first conclusion of potential interest: Arias intensity cannot alone be a reliable predictor of slip, especially with motions containing acceleration pulses of large duration ('directivity' or, especially, 'fling' related). Thus, for example the Lucerne record, despite its I_A two times larger than the TCU-068 record, leads to permanent slip that is four to eight times smaller. This implies (in total) more than an order of magnitude 'error', had I_A been used for prediction of the potential repercussions of the two motions. This conclusion is in accord with the observation by Sarma & Kourkoulis (2004) and Crespellani *et al.* (1998). The latter proposed for slope deformation a corrected measure of motion 'destructiveness' based on Arias intensity along with the average rate of zero-crossing of the record. This raises questions on the applicability of empirical correlations between D_{res} and I_A such as those presented by Jibson (1994) and Del Gaudio *et al.* (2003). Further discussion on this topic, however, is well beyond the scope of the current paper.

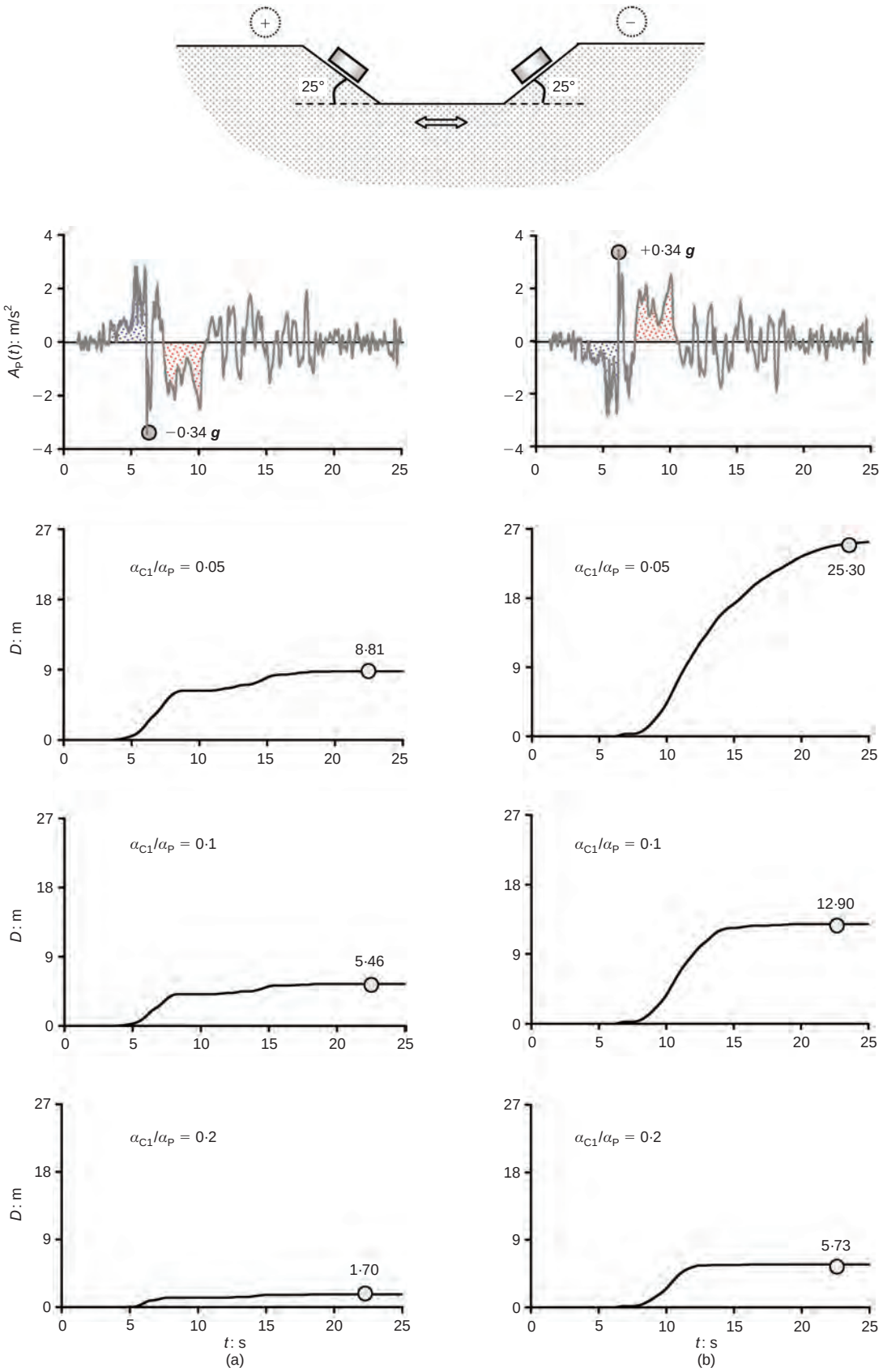

Fig. 15. Effect of reversing polarity of the TCU 068-NS record upon the slip on a 25° sloping plane, for three different α_{C1}/α_P ratios

CONCLUSIONS

(*a*) The asymmetric sliding of a rigid mass subjected to base excitation serves as a model for a variety of geotechnical and structural earthquake problems, such as retaining walls, slopes and landslides, dams and embankments, friction-supported structures restrained on one side by stoppers or adjacent structures, and so on.

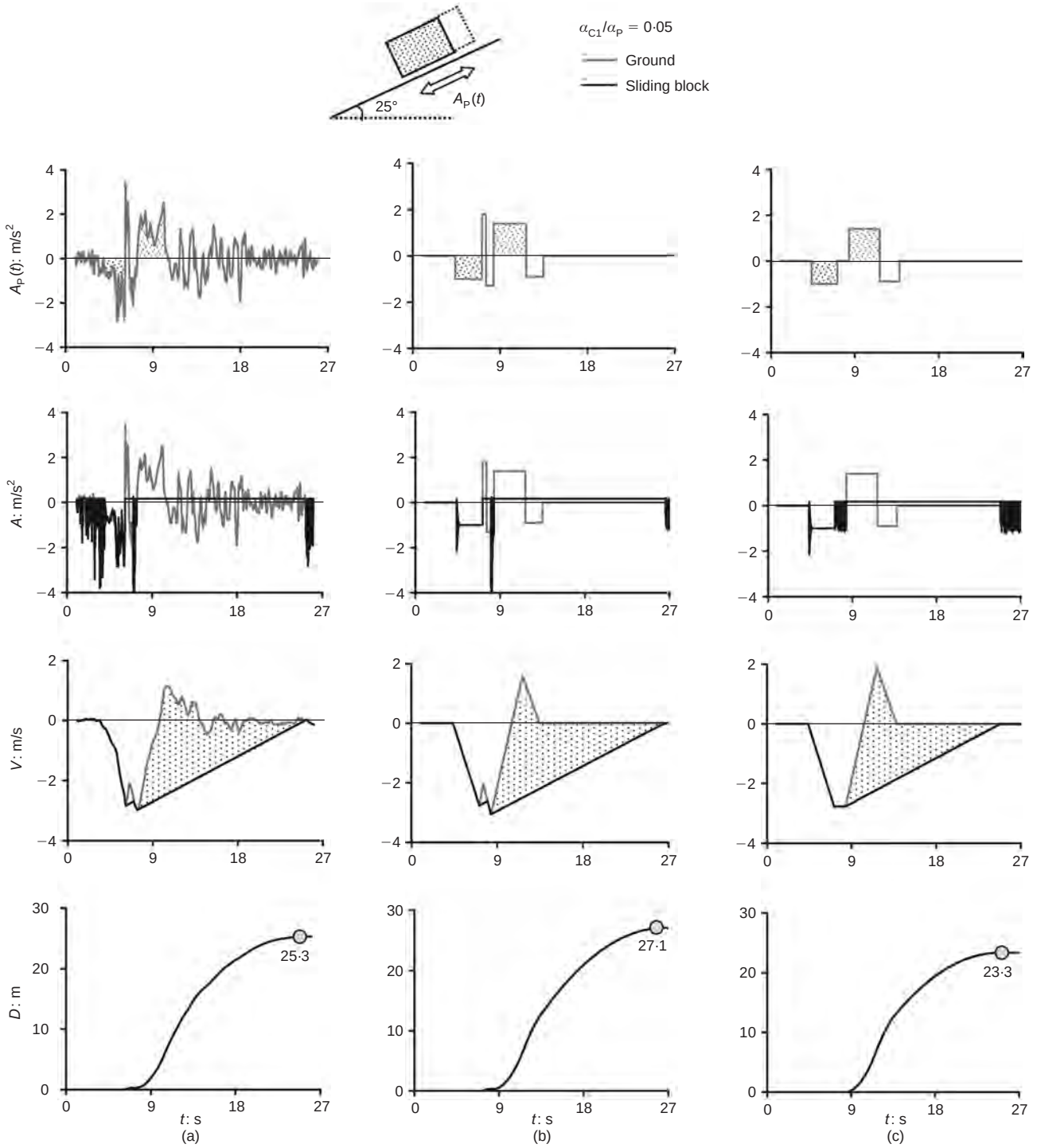

Fig. 16. Simulation of the TCU 068-NS record through a series of simple rectangular pulses. (a) The real record and its consequences on block acceleration, velocity and slippage. (b) Approximation of the record with five rectangular pulses (representing almost every major acceleration pulse of the record) and its consequences on block response. (c) Approximation of the record with only three rectangular pulses (representing only the long-period pulses of the record) and its consequences on block response. The final accumulated slip values in all three cases are quite similar, an indirect evidence of the dominating role of the long acceleration pulses and the minor importance of the isolated 'spikes' of peak ground acceleration

(*b*) The graphical solutions portrayed in the paper (through the acceleration and velocity–time histories of the base (input) and the mass (output)) are easy to understand, offering considerable insight into the dynamics of asymmetric sliding.

(*c*) Forward-directivity- and fling-step-affected motions, containing 'severe' acceleration pulses and/or large velocity steps, may have a profound and unpredictably detrimental effect on residual slip, especially for small values of the critical (threshold) acceleration (or, equivalently, for small coefficient of friction). The characterisation as 'unpredictable' is justified on at least two counts:

- in view of the proven sensitivity of the slip not only to peak acceleration and peak velocity of the record but, most significantly, to the sequence, duration, and phasing of the main pulses (the 'details' of motion)
- in light of the underprediction of the residual slip by many of the currently popular charts and diagrams.

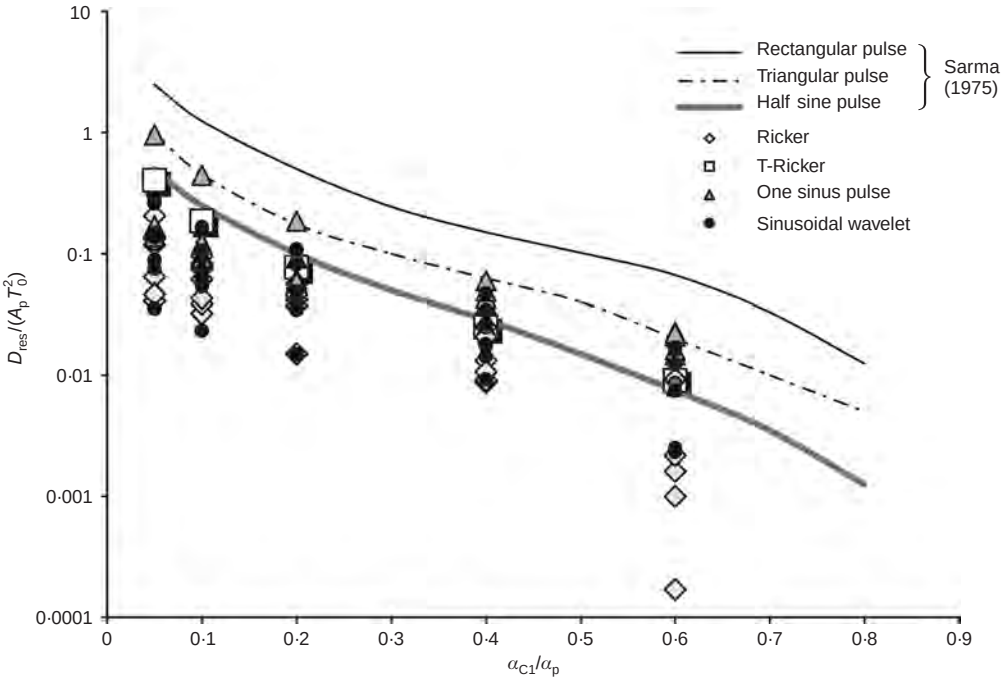

Fig. 17. Comparison of the normalised slip triggered by idealised wavelets computed in the present study with the published results of Sarma (1975) for typical simple pulses. Understandably, the single rectangular pulse triggers always the largest slippage

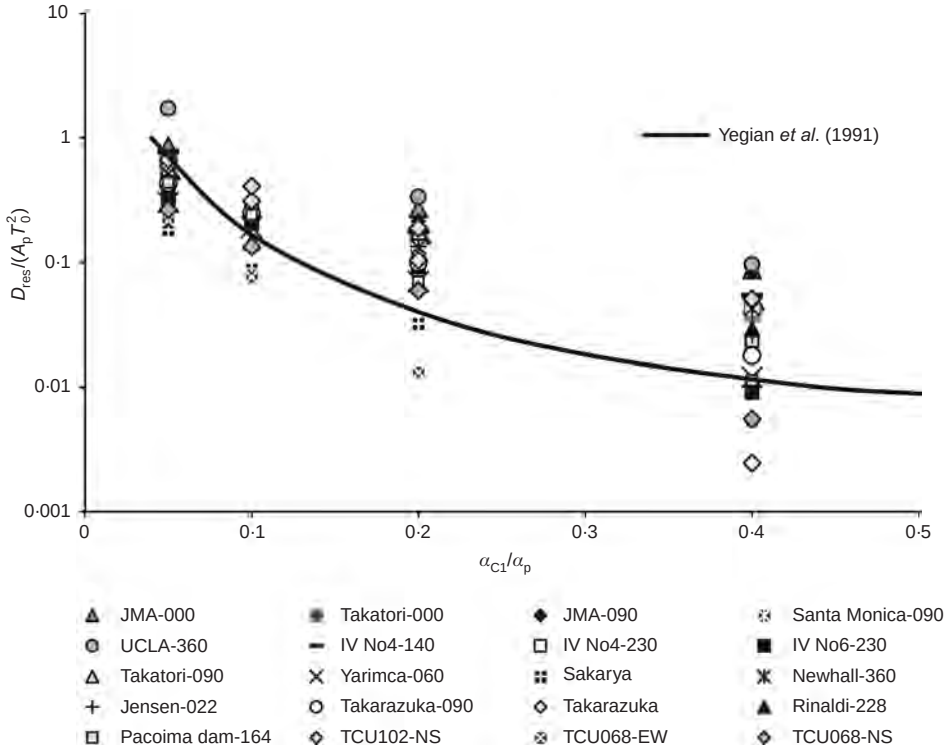

Fig. 18. Comparison of the published dimensionless results of Yegian *et al.* (1991) with the normalised slippage computed in this paper with all the 20 records. The Yegian curve refers to a 50% probability of exceedance

(*d*) Changing the polarity of excitation (i.e. applying it in the + and then in the − direction) may have a most dramatic effect on the accumulating slip. The reader should reflect on the potential significance if this finding in post-seismic field reconnaissance investigations, when, while documenting the performance of neighbouring, very similar retaining walls, slopes or other strongly inelastic systems, she/he is confronted with inexplicably large differences 'across the street'.

(*e*) Finally, comparison between the numerical results presented in the paper and the charts available in the literature, shows that while the dimensionless diagrams

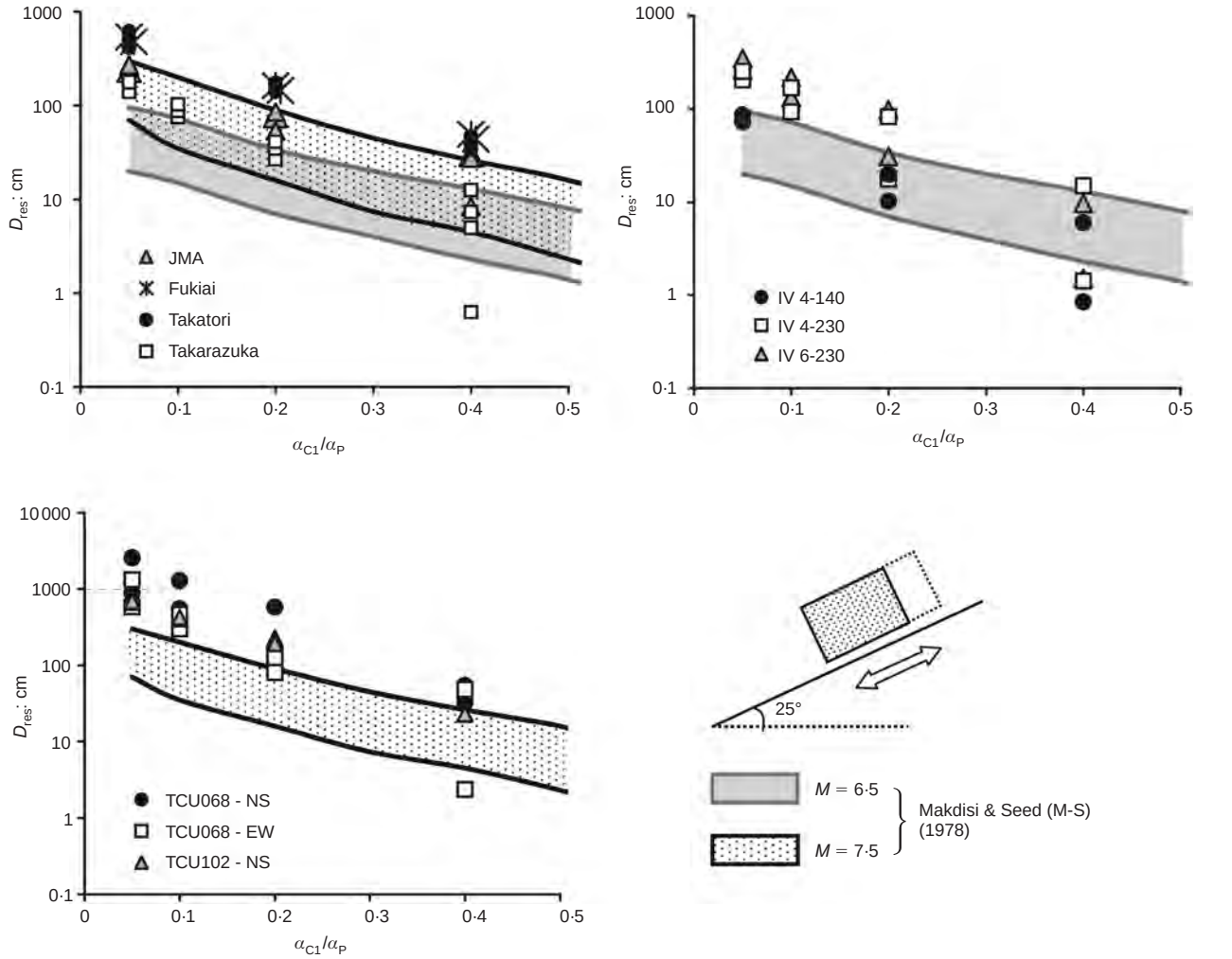

Fig. 19. Comparison of the widely used results of Makdisi & Seed (1978) with the computed sliding response induced by: the Kobe records (top left), the Imperial Valley records (top right), and the Chi-Chi records (bottom left). Each excitation is imposed with the + and − polarity. Evidently, some of the severe near-fault records utilised lead to much larger slip, especially at small α_{C1}/α_P ratios. For the Chi-Chi records the superiority reaches one order of magnitude

> of Yegian *et al.* (1991) describe quite well the extreme slippage at small values of the critical acceleration ratio, α_{C1}/α_P , the Makdisi & Seed (1978) charts that are presently enjoying widespread use will usually (but justifiably) underestimate the slippage caused by near-fault 'severe' ground motions – in some cases substantially.

The results of this study can be used as a guide for a safe analysis of strongly inelastic systems near major seismic faults. Alternatively, the conclusion of Kramer & Lindwall (2004) could be adopted, that

> because [sliding] displacements are influenced by the details of the input motion, including the phasing of the various components, stable estimates of permanent displacement will require analyses of suites of input motions.

To answer the question that seismologists have repeatedly raised (e.g. Abrahamson, 2001), both directivity and fling effects can be very significant for structural and geotechnical systems – especially if the seismic behaviour of the latter is strongly inelastic, as are the rigid–perfectly-plastic systems (sliding blocks) investigated in this paper.

ACKNOWLEDGEMENT

The work of this paper was conducted for the project 'DARE', financed by a European Research Council (ERC) advanced grant under the 'Ideas' Programme in Support of Frontier Research (grant agreement 228254).

NOTATION

$A_{C1} = \alpha_{C1}g$	critical (threshold) yielding acceleration of the block for sliding downward
$A_{C2} = \alpha_{C2}g$	critical (threshold) yield acceleration of the block upward
$A_P = \alpha_P g$	peak value of the ground acceleration $A_P(t)$ applied parallel to the slope
$D(t)$, D_m	sliding displacement time history and maximum sliding displacement from a single pulse
D_{res}	residual (permanent) sliding displacement
f_o	dominant frequency of ground excitation
I_A	Arias intensity (see equation (4))
M	earthquake magnitude
T_o	dominant period of ground motion
V_P	peak ground velocity of the excitation applied parallel to the slope
β	angle of the inclined plane measured from the horizontal
ΔV	maximum velocity step (Bertero *et al.*, 1978)
μ	Coulomb's constant coefficient of friction

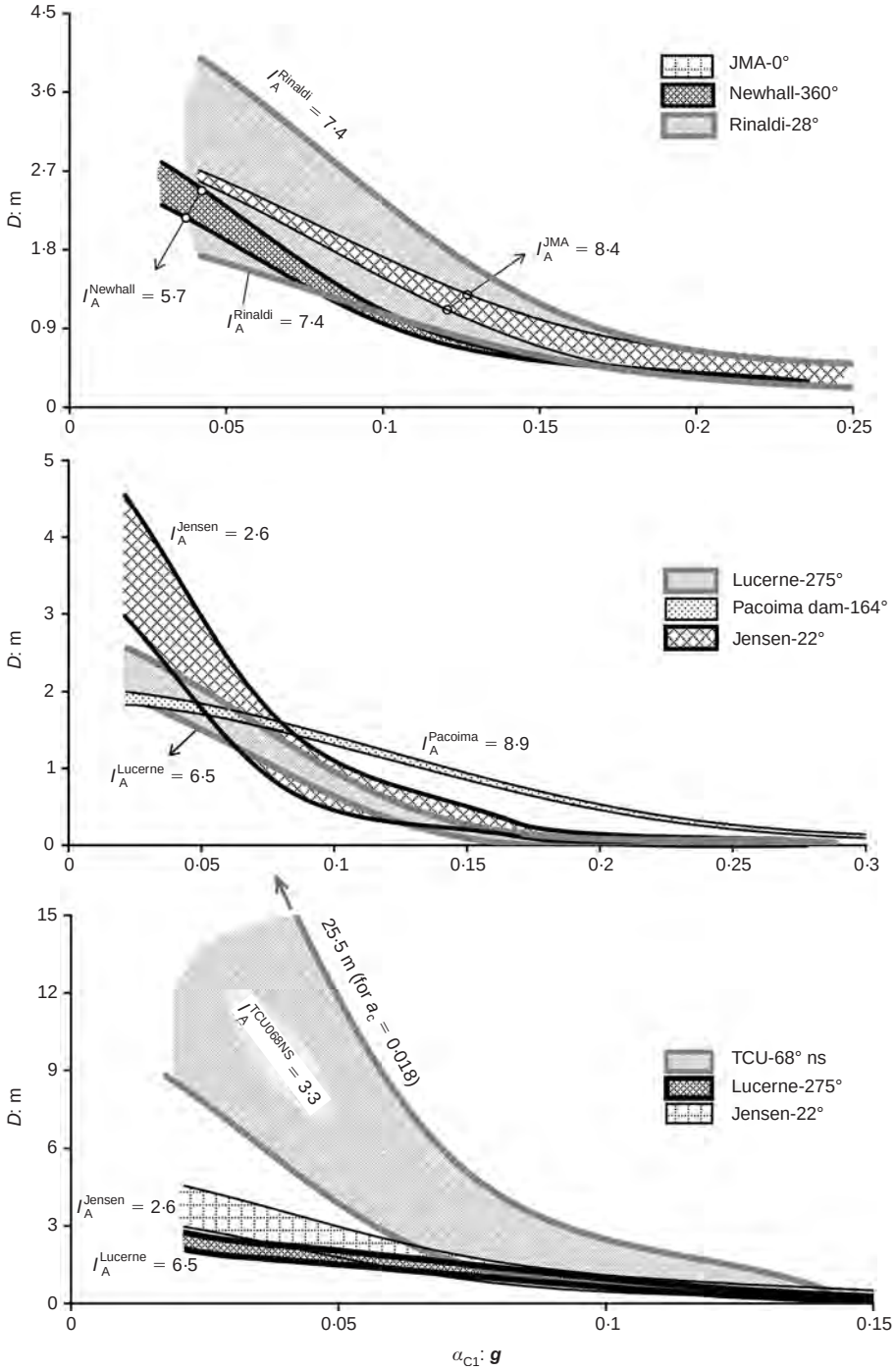

Fig. 20. Induced slippage with respect to critical acceleration for several groups of records imposed with both polarities. No convincing correlation could be found between the accumulated slip and the Arias intensity, I_A, of the records. A 'mere' reversal of polarity, while leaving I_A unchanged, may lead to differences by a factor of 3 or more

REFERENCES

Abrahamson, N. A. (2000). Effects of rupture directivity on probabilistic seismic hazard analysis. *Proc. 6th Int. Conf. Seismic Zonation, Palm Springs, California* **1**, 151–156. Oakland, CA: Earthquake Engineering Research Institute.

Abrahamson, N. A. (2001). *Incorporating effects of near fault tectonic deformation into design ground motions*. University at Buffalo MCEER: Friedman F. V. Professional Program, webcast, see http://mceer:buffalo.edu/outreach/pr/Abrahamson.asp for further details.

Abrahamson, N. A. & Shedlock, M. K. (1997). Overview. *Seismol. Res. Lett*. **68**, No. 1, 9–23.

Alavi, B. & Krawinkler, H. (2000). Consideration of near-fault ground motion effects in seismic design. *Proc. 12th World Earthquake Conf. on Earthquake Engng, New Zealand*, paper no. 2665 (CD-ROM).

Ambraseys, N. N. & Sarma, S. K. (1967). The response of earth dams to strong earthquakes. *Géotechnique* **17**, No. 2, 181–213, **doi**: 10.1680/geot.1967.17.2.181.

Ambraseys, N. N. & Menu, J. (1988). Earthquake induced ground displacements. *Earthquake Engng Struct. Dynamics* **16**, No. 7, 985–1006.

Ambraseys, N. N. & Srbulov, M. (1994). Attenuation of earthquake-induced ground displacements. *Earthquake Engng Struct. Dynamics* **23**, No. 5, 467–487.

Bertero, V. V. (1976). Establishment of design earthquakes: evaluation of present methods. *Proceedings of the international symposium of earthquake structural engineering*, University of

Missouri-Rolla, St Louis, Vol. 1, pp. 551–580.
Bertero, V. V., Mahin, S. A. & Herrera, R. A. (1978). Aseismic design implications of near-fault San Fernando earthquake records. *Earthquake Engng Struct. Dynamics* **6**, No. 1, 31–42.
Bolt, B. A. (2004). *Earthquakes*, 5th edn. New York: W. H. Freeman.
Boore, M. D. (2001). Effect of baseline corrections on displacements and response spectra for several Recordings of the 1999 Chi-Chi, Taiwan, earthquake. *Bull. Seismol. Soc. Am*. **91**, No. 5, 1199–1211.
Bray, J. D. & Rathje, E. M. (1998). Earthquake-induced displacements of solid-waste landfills. *J. Geotech. Geoenviron. Engng, ASCE* **124**, No. 3, 242–253.
Bray, J. D. & Rodriguez-Marek, A. (2004). Characterization of forward–directivity ground motions in the near-fault region. *Soil Dynamics Earthquake Engng* **24**, No. 11, 815–828.
Changhai, Z., Shuang, L., Xie, L. L. & Yamin, S. (2007). Study on inelastic displacement ratio spectra for near-fault pulse-type ground motions. *Earthquake Engng and Engng Vibr.* **6**, No. 4, 351–356.
Constantinou, M. C. & Gazetas, G. (1987). Probabilistic seismic sliding deformations of earth dams and slopes. *Proceedings of the specialty conference on probabilistic mechanics and structural reliability*, ASCE, Berkeley, pp. 318–321.
Constantinou, M. C., Gazetas, G. & Tadjbakhsh, I. (1984). Stochastic seismic sliding of rigid mass against asymmetric coulomb friction. *Earthquake Engng Struct. Dynamics* **12**, No. 7, 777–793.
Crespellani, T., Madiai, C. & Vannucchi, G. (1998). Earthquake destructiveness potential factor and slope stability. *Géotechnique* **48**, No. 3, 411–420, **doi**: 10.1680/geot.1998.48.3.411.
Dakoulas, P. & Gazetas, G. (2008). Insight into seismic earth and water pressures against caisson quay walls. *Géotechnique* **58**, No. 2, 95–111, **doi**: 10.1680/geot.2008.58.2.95.
Danay, A. & Adeghe, L. N. (1993). Seismic induced slip of concrete gravity dams. *J. Struct. Engng, ASCE* **119**, No. 1, 108–1129.
Del Gaudio, V., Pierri, P. & Wasowski, J. (2003). An approach to time-probabilistic evaluation of seismically induced landslide hazard. *Bull. Seismol. Soc. Am*. **93**, No. 2, 557–569.
Fardis, N., Georgarakos, P., Gazetas, G. & Anastasopoulos, I. (2003). Sliding isolation of structures: effect of horizontal and vertical acceleration. *Proceedings of the FIB international symposium on concrete structures in seismic regions*, Athens, Greece (on CD-ROM).
Fenves, G. & Chopra, A. K. (1986). *Simplified analysis for earthquake resistant design of concrete gravity dams*, Report UBC/EERC-85/10. Berkeley: University of California.
Franklin, A. & Chang, F. K. (1977). *Earthquake resistance of earth and rock-fill dams*, Report 5: permanent displacements of earth embankments by Newmark sliding block analysis, miscellaneous paper S-71-17. Vicksburg, MS: Soils and Pavements Laboratory, US Army Engineer Waterways Experiment Station.
Gazetas, G, Garini, E., Anastasopoulos, I. & Georgarakos, T. (2009). Effects of near-fault ground shaking on sliding systems. *J. Geotech. Geoenviron. Engng, ASCE* **135**, No. 12, 1906–1921.
Gazetas, G. (1996). *Soil dynamics and earthquake engineering: case histories*, ch. 5 'The Aegion 1995 earthquake', pp. 269–317. Athens, Greece: Symeon Publishers.
Gazetas, G. & Uddin, N. (1994). Permanent deformation on preexisting sliding surfaces in dams. *J. Geotech. Engng, ASCE* **120**, No. 11, 2041–2061.
Gazetas, G., Debchaudhury, A. & Gasparini, D. A. (1981). Random vibration analysis for the seismic response of earth dams. *Géotechnique* **31**, No. 2, 261–277.
Hall, J. F., Heaton, T. H., Halling, M. W. & Wald, D. J. (1995). Near-source ground motion and its effects on flexible buildings. *Earthquake Spectra* **11**, No. 4, 569–605.
Hamada, M. & Wakamatsu, K. (1996). Liquefaction, ground deformation and their caused damage to structures. In *The 1995 Hyogoken-Nanbu earthquake* (ed. Committee of Earthquake Engineering), pp. 45–91. Tokyo: Japan Society of Civil Engineers.
Hamada, M., Isoyama, R. & Wakamatsu, K. (1995). *The 1995 Hyogoken-Nanbu (Kobe) earthquake: liquefaction, ground displacement and soil condition in Hanshin area*. Japan: Association for Development of Earthquake Prediction.
Harp, E. L. & Jibson, R. W. (1995). Seismic instrumentation of landslides: Building a better model of dynamic landslide behaviour. *Bull. Seismol. Soc. Am*. **85**, No. 1, 93–99.
Harp, E. L. & Wilson, R. C. (1995). Shaking intensity thresholds for rock falls and slides: evidence from 1987 Whittier Narrows and Superstition Hills earthquakes, strong motion records. *Bull. Seismol. Soc. Am*. **85**, No. 6, 1739–1757.
Hisada, Y. & Bielak, J. (2003). A theoretical method for computing near-fault ground motions in layered half-spaces considering static offset due to surface faulting, with a physical interpretation of fling step and rupture directivity. *Bull. Seismol. Soc. Am*. **93**, No. 3, 1154–1168.
Howard, J. K., Tracy, C. A. & Burns, R. G. (2005). Comparing observed and predicted directivity in near-source ground motion. *Earthquake Spectra* **21**, No. 4, 1063–1092.
Huang, C. C., Lee, Y. H., Liu, H. P., Keefer, D. K. & Jibson, R. W. (2001). Influence of surface-normal ground acceleration on the initiation of the Jih-Feng-Erh-Shan landslide during the 1999 Chi-Chi, Taiwan, earthquake. *Bull. Seismol. Soc. Am*. **91**, No. 5, 953–958.
Ishihara, K. (1997). Terzaghi oration: geotechnical aspects of the 1995 Kobe Earthquake. *Proc. 14th Conf. Soil Mech. Found. Engng, Hamburg* **4**, 2047–2073.
Iwan, W. D., Huang, C. T. & Guyader, A. C. (2000). Important features of the response of inelastic structures to near-fault ground motion. *Proc. 12th World Earthquake Conf. Earthquake Engng, Auckland, New Zealand*, paper no. 1740 (CD-ROM).
Jibson, R. (1994). Predicting earthquake-induced landslide displacements using Newmark's sliding block analysis. *Transportation Res. Rec.*, No. 1411, pp. 9–17.
Junwu, D., Tong, M., Lee, G.C., Xiaorhai, Q. & Wenting, B. (2004). Dynamic responses under the excitation of pulse sequences. *Earthquake Engng and Engng Vibr.* **3**, No. 2, 157–169.
Kramer, S. L. (1996). *Geotechnical earthquake engineering*. Prentice-Hall.
Kramer, S. L. & Lindwall, N. W. (2004). Dimensionality and directionality effects of Newmark stability analysis. *J. Geotech. Geoenviron. Engng, ASCE* **130**, No. 3, 303–315.
Kramer, S. L. & Smith, M. (1997). Modified Newmark model for seismic displacements of compliant slopes. *J. Geotech. Geoenviron. Engng, ASCE* **123**, No. 7, 635–644.
Leger, P. & Katsouli, M. (1989). Seismic stability of concrete gravity dams, *Earthquake Engng Struct. Dynamics* **18**, No. 8, 889–902.
Lin, J. S. & Whitman, R. V. (1983). Decoupling approximation to the evaluation of earthquake-induced plastic slip in earth dams. *Earthquake Engng Struct. Dynamics* **11**, No. 6, 667–678.
Ling, H. (2001). Recent applications of sliding block theory to geotechnical design. *Soil Dynamics Earthquake Engng, ASCE* **21**, No. 3, 189–197.
Makdisi, F. I. & Seed, H. B. (1978). Simplified procedure for estimating dam and embankment earthquake induced deformations. *J. Geotech. Engng Div., ASCE* **104**, No. 7, 849–867.
Makris, N. & Psychogios, T. (2006). Dimensional response analysis of yielding structures with first mode dominated response. *Earthquake Engng Struct. Dynamics* **35**, No. 11, 1203–1224.
Makris, N. & Roussos, Y. S. (2000). Rocking response of rigid blocks under near-source ground motions. *Géotechnique* **50**, No. 3, 243–262, **doi**: 10.1680/geot.2000.50.3.243.
Marcuson, W. F. (1994). An example of professional modesty. In *The Earth, Engineers, and Education: A Symposium in Honor of Robert V. Whitman*. Cambridge, MA, USA: Massachusetts Institute of Technology.
Mavroeidis, P.G. & Papageorgiou, S. A. (2003). A mathematical representation of near-fault ground motions. *Bull. Seismol. Soc. Am*. **93**, No. 3, 1099–1131.
Mavroeidis, P. G. & Papageorgiou, S. A. (2010). Effect of fault rupture characteristics on near-fault strong ground motions. *Bull. Seismol. Soc. Am*. **100**, No. 1, 37–58.
Mavroeidis, P. G., Dong, G. & Papageorgiou, S. A. (2004). Near-fault ground motions, and the response of elastic and inelastic single-degree-of-freedom (SDOF) systems. *Earthquake Engng Struct. Dynamics* **33**, No. 9, 1023–1049.
Newmark, N. M. (1965). Effects of earthquakes on dams and

embankments, *Géotechnique* **15**, No. 2, 139–160, **doi**: 10.1680/geot.1965.15.2.139.

Pavlou, E. A. & Constantinou, M. C. (2004). Response of elastic and inelastic structures with damping systems to near-field and soft-soil ground motions. *Engng Structs* **26**, No. 9, 1217–1230.

Pitarka, A., Somerville, P. G., Fukushima, Y., Uetake, T. & Irikura, K. (2000). Simulation of near-fault strong-ground motion using hybrid Green's functions. *Bull. Seismol. Soc. Am*. **90**, No. 3, 566–586.

Pitarka, A., Somerville, P. G., Fukushima, Y. & Uetake, T. (2002). Ground-motion attenuation from the 1995 Kobe earthquake based on simulations using the hybrid green's function method. *Bull. Seismol. Soc. Am*. **92**, No. 3, 1025–1031.

Rathje, E. M. & Bray, J. D. (1999). An examination of simplified earthquake-induced displacement procedures for earth structures. *Can. Geotech. J*. **36**, No. 1, 72–87.

Rathje, E. M. & Bray, J. D. (2000). Nonlinear coupled seismic sliding analysis of earth structures. *J. Geotech. Geoenviron. Engng, ASCE* **126**, No. 11, 1002–1014.

Reitherman, R. (2010). *Connections: Robert V. Whitman*, Oral History Series. Berkeley, California: Earthquake Engineering Research Institute.

Richards, R. & Elms, D. G. (1979). Seismic behaviour of gravity retaining walls. *J. Geotech. Engng Div., ASCE* **105**, No. 4, 449–464.

Richards, R., Elms, D. G. & Budhu, M. (1993). Seismic bearing capacity and settlement of foundations. *J. Geotech. Engng ASCE* **119**, No. 4, 662–674.

Sarma, S. K. (1975). Seismic stability of earth dams and embankments. *Géotechnique* **25**, No. 4, 743–761, **doi**: 10.1680/geot.1975.25.4.743.

Sarma, S. K. (1981). Seismic displacement analysis of earth dams. *J. Geotech. Engng Div., ASCE* **107**, No. 12, 1735–1739.

Sarma, S. K. & Kourkoulis, R. (2004). Investigation into the prediction of sliding block displacements in seismic analysis of earth dams. *Proc. 13th World Conf. Earthquake Engng, Vancouver, Canada*, paper no. 1957 (CD-ROM).

Sarma, S. K. & Scorer, M. (2009). The effect of vertical accelerations on seismic slope stability. *Proceedings of the international conference on performance based design in earthquake geotechnical engineering* (eds T. Kokusho, U. Tsukamoto & M. Yoshimine), IS-Tokyo 2009, on CD rom, p. 889.

Sasani, M. & Bertero, V. V. (2000). Importance of severe pulse-type ground motions in performance-based engineering: historical and critical review. *Proc. 12th World Conf. Earthquake Engng, Auckland, New Zealand*, paper no. 1302 (CD-ROM).

Sawada, T., Chen, W. F. & Nomachi, S. G. (1993). Assessment of seismic displacements of slopes. *Soil Dynamics Earthquake Engng* **12**, No. 6, 357–362.

Seed, H. B. & Martin, G. R. (1966). The seismic coefficient in earth dam design, *J. Soil Mech. Found. Div.*, *ASCE* **92**, No. 1, 25–58.

Singh, J. P. (1985). Earthquake ground motions: implications for designing structures and reconciling structural damage, *Earthquake Spectra*, Vol. 1, No. 2, 239–270.

Somerville, P. (2000). Seismic hazard evaluation. *12th WCEE 2000, Bull. New Zealand Soc. Earthquake Engng* **33**, No. 1, 325–346, 484–491.

Somerville, P. (2003). Characterization of near fault ground motions for design. *Proceedings of the ACI specialty conference*, University of California, San Diego. American Concrete Institute.

Somerville, P. G., Saikia, C., Wald, D. & Graves, R. (1996). Implications of the Northridge earthquake for strong ground motions from thrust faults. *Bull. Seismol. Soc. Am*. **86**, No. 1, 115 – 125.

Somerville, P. G., Smith, N. F., Graves, R. W. & Abrahamson, N. A. (1997). Modification of empirical strong ground motion attenuation relations to include the amplitude and duration effects of rupture directivity. *Seismol. Res. Lett*. **68**, No. 1, 199–222.

Stamatopoulos, C. A. (1996). Sliding system predicting large permanent co-seismic movements of slopes. *Earthquake Engng Struct. Dynamics* **25**, No. 10, 1075–1093.

Taflampas, I. (2009). *Evaluation of strong ground motion in engineering seismology and structural vulnerability.* PhD thesis, National Technical University, Athens, Greece.

Travasarou, T. (2003). *Optimal ground motion intensity measures for probabilistic assessment of seismic slope displacements*. PhD thesis, Civil and Environmental Engineering, University of California, Berkeley.

Voyagaki, E. L., Mylonakis, G. E. & Psycharis, I. N. (2008a). Sliding response of rigid blocks on inclined plane under idealised near-fault pulses. *Proc. 3rd Natn. Conf. Earthquake Engng and Engng Seismol*., *Athens* (ed. G. Gazetas) paper no. 1908 (CD-ROM). Athens, Greece: Hellenic Society for Earthquake Engineering.

Voyagaki, E. L., Mylonakis, G. E. & Psycharis, I. N. (2008b). Sliding blocks under near-fault pulses: closed form solutions. In *Geotechnical Earthquake Engineering and Soil Dynamics IV* (eds D. Zeng, M. T. Manzari and D. R. Hiltunen), ASCE Geotechnical Special Publication No. 181. Reston, VA: American Society of Civil Engineers.

Wartman, J., Bray, J. D. & Seed, R. B. (2003). Inclined plane studies of the Newmark sliding block procedure. *J. Geotech. Geoenviron. Engng, ASCE* **129**, No. 8, 673–684.

Wilson, R. C. & Keefer, D. K. (1983). Dynamic analysis of a slope failure from the 6 August, 1979 Coyote Lake, California earthquake. *Bull. Seismol. Soc. Am*. **73**, No. 3, 863–877.

Xie, L. L., Xu, L. J. & Rondriguez-Marek, A. (2005). Representation of near-fault pulse-type ground motions. *Earthquake Engng and Engng Vibr*. **4**, No. 2, 191–199.

Xu, L. J., Rondriguez-Marek, A. & Xie, L. L. (2006). Design spectra including effect of rupture directivity in near-fault region. *Earthquake Engng and Engng Vibr*. **5**, No. 2, 159–170.

Yegian, M. K. & Lahlaf, A. M. (1992). Dynamic interface shear strength properties of geomembranes and geotextiles. *J. Geotech. Engng, ASCE* **118**, No. 5, 760–761.

Yegian, M. K., Marciano, E. A. & Ghahraman, V. G. (1991). Earthquake induced permanent deformations: a probabilistic approach. *J. Geotech. Engng, ASCE* **117**, No. 1, 35–50.

Yegian, M. K., Harb, J. N. & Kadakal, U. (1998). Dynamic response analysis procedure for landfills and geosynthetic liners. *J. Geotech. Geoenviron. Engng, ASCE* **124**, No. 10, 1027–1033.